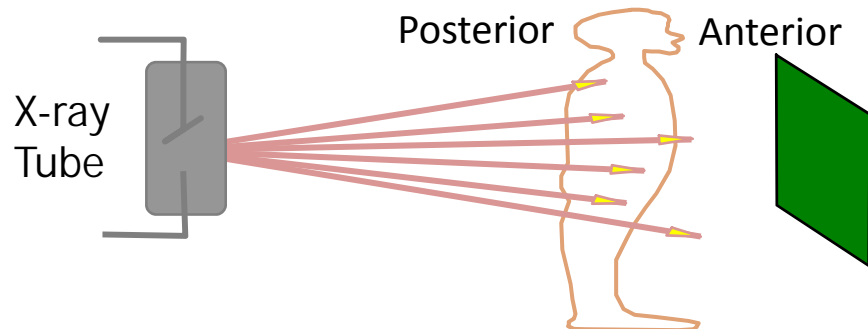


## Handout # 6 X-ray Tomography

### 6.1 X-ray Computed Tomography

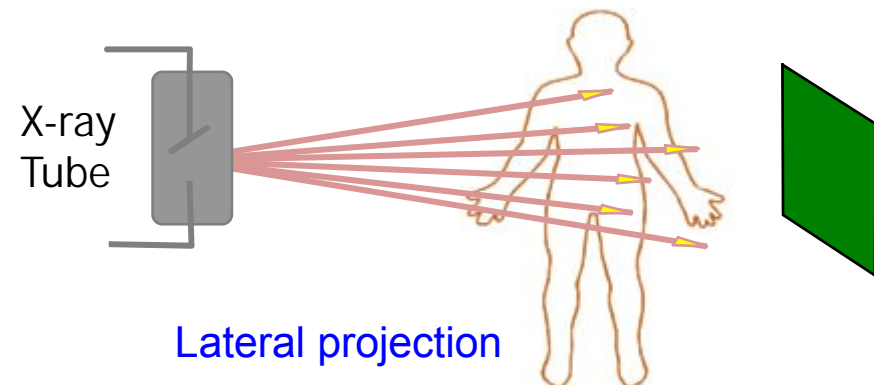
#### (1) Basic principle

- ❖ Limitation of 2D projection radiography: depth information is lost
- ❖ Posterior-anterior (PA) and lateral projections: provide limited location information.



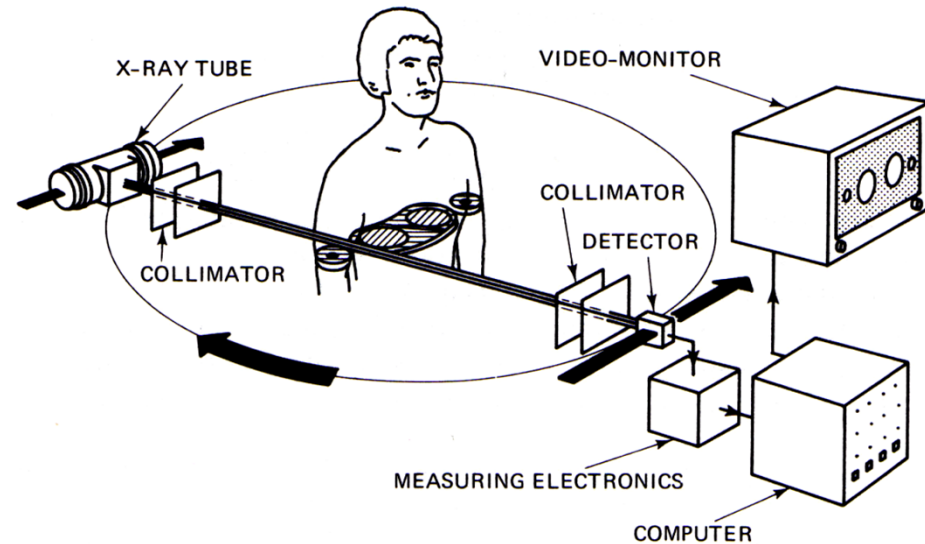
Posterior-Anterior (PA) projection

Lateral projection: X-ray beam passes the patient from the left side to the right side, or vice versa.



Lateral projection

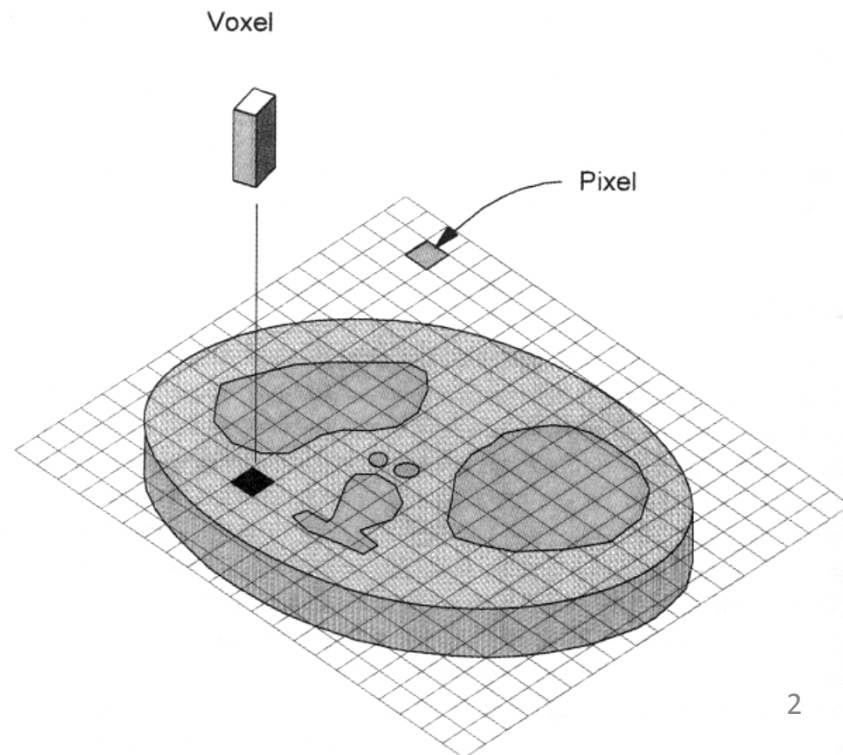
- ❖ Computed tomography:  
Computed tomography maps the linear attenuation coefficients throughout a transverse slice of tissue (or an object).



- ❖ Computed tomography:  
**Concepts of pixel and voxel**

**Pixel:** Picture element

**Voxel:** Volume element



## (2) Data acquisition

**What do we measure in a 2D projection?**

$$\begin{aligned} N_0 &= N_i e^{-\mu x} \\ &= N_i e^{-(\mu_1 + \mu_2 + \dots) \Delta x} \end{aligned}$$

The output signal is dependent of exposure technique

**What do we measure in CT projection (Ray sums) ?**

### Ray-Sum X-ray Attenuation



$$N_o = N_i e^{-\sum_k \mu_k \Delta x}$$

**Ray-sum**

$$\sum_k \mu_k \Delta x = \ln \frac{N_i}{N_o}$$

**Line integral**

$$\int_{-\infty}^{\infty} \mu(x) dx = \ln \frac{N_i}{N_o}$$

In data acquisition, one measures  **$p$  ( $N_i$  and  $N_0$ )** using detectors.

$$p = \ln\left(\frac{N_i}{N_0}\right) = \mu x = \sum_k \mu_k \Delta x = (\mu_1 + \mu_2 + \mu_3 + \dots) \Delta x$$

With measured  **$p$**  values, the image reconstruction process in CT determines the linear attenuation coefficient,  $\mu_1, \mu_2, \mu_3, \dots$  associated with each **voxel**.

**What do we display ?**

**CT number: Re-scaled linear attenuation coefficients**

$$CT\ number = 1000 \times (\mu - \mu_{water}) / \mu_{water} \quad \text{(Hounsfield unit)}$$

Pixel values of a reconstructed CT image indicate **relative (to water), rather than absolute, linear attenuation coefficients**.

### Exercise-1:

A liver is imaged by a CT system. Assume a mono-energetic x-ray source, for which the linear attenuation coefficients of water and liver are:  $\mu_{water} = 0.2 \text{ cm}^{-1}$  and  $\mu_{liver} = 0.215 \text{ cm}^{-1}$  respectively. What is the CT number of the liver under the same mono-energetic x-ray source?

### Exercise-1:

A liver is imaged by a CT system. Assume a mono-energetic x-ray source, for which the linear attenuation coefficients of water and liver are:  $\mu_{water} = 0.2 \text{ cm}^{-1}$  and  $\mu_{liver} = 0.215 \text{ cm}^{-1}$  respectively. What is the CT number of the liver under the same mono-energetic x-ray source?

### Solution:

$$CT \text{ number} = 1000 \times (\mu - \mu_{water}) / \mu_{water}$$

The CT number of the liver:

$$CT \text{ number} = 1000 \times \frac{\mu_{liver} - \mu_{water}}{\mu_{water}} = 1000 \times \frac{0.215 - 0.2}{0.2} = 75$$

**Representative CT numbers (for an x-ray beam in the range of 120 to 140KVp)**

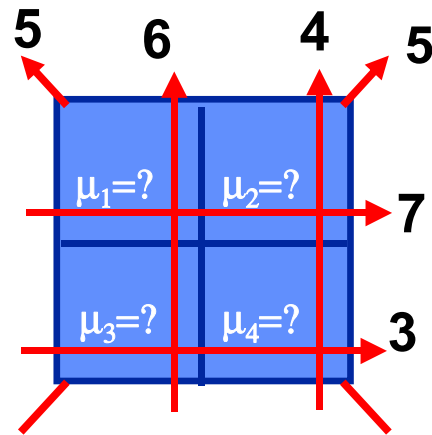
| <b>Subject/tissue</b> | <b>CT number</b> |
|-----------------------|------------------|
| Water                 | 0                |
| Air                   | -1000            |
| Dense Bone            | About 1000       |
| Blood                 | 42 to 58         |
| Blood Clot            | 74 to 81         |
| Heart                 | 24               |
| Muscle                | 44 to 59         |
| Fat                   | -20 to -100      |
| Lung                  | -300             |

From Webster JG, ed. Encyclopedia of Medical Devices and Instrumentation, New York, Wiley, 1988, P. 834

### (3) Reconstruction techniques

#### (a) Basic reconstruction idea

##### Reconstruction Idea

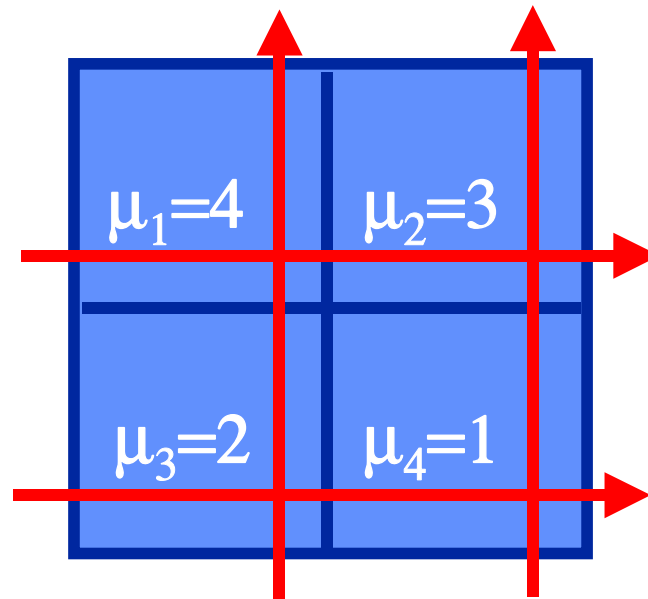


$$\begin{cases} \mu_1 + \mu_2 = 7 \\ \mu_3 + \mu_4 = 3 \\ \mu_1 + \mu_3 = 6 \\ \mu_2 + \mu_4 = 4 \end{cases}$$

$$\mu_2 + \mu_3 = 5$$

$$\mu_1 + \mu_4 = 5$$

**Solution:**



**Here we assume the  
voxel dimension  $\Delta x=1$**



## (b) Iterative approaches

### ---Algebraic reconstruction technique (ART)

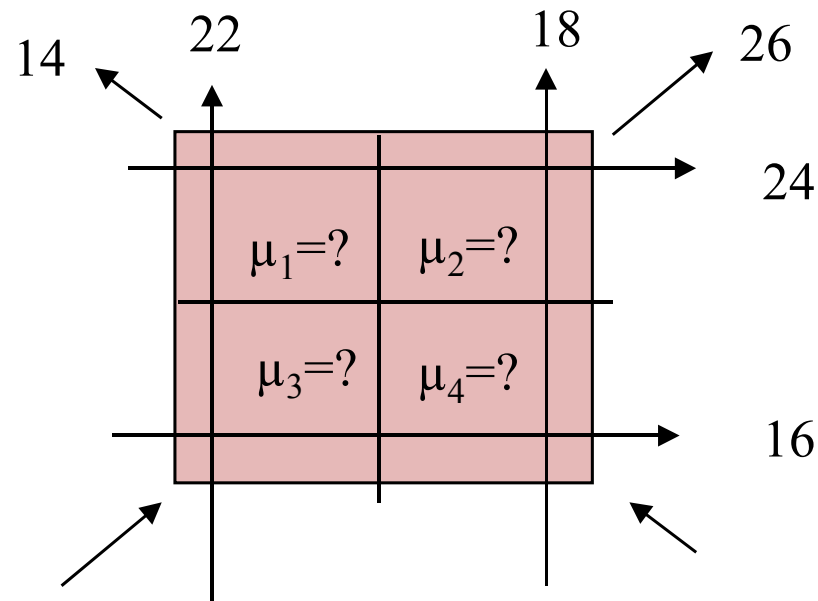
First set all reconstruction element  $\mu_i$ , to a constant, such as 0. In each iteration, the difference between the measured ray sum ( $p$ ) and the **sum of the reconstructed elements** along that ray  $\sum \mu_i$  is calculated. This difference is then divided by  $N$ , number of elements along the ray. Superscript  $q$  indicates the iteration.

$$\mu_i^{(q+1)} = \mu_i^{(q)} + \frac{p - \sum \mu_i^{(q)}}{N}$$

**Here we assume the voxel dimension  $\Delta x=1$**

### Example:

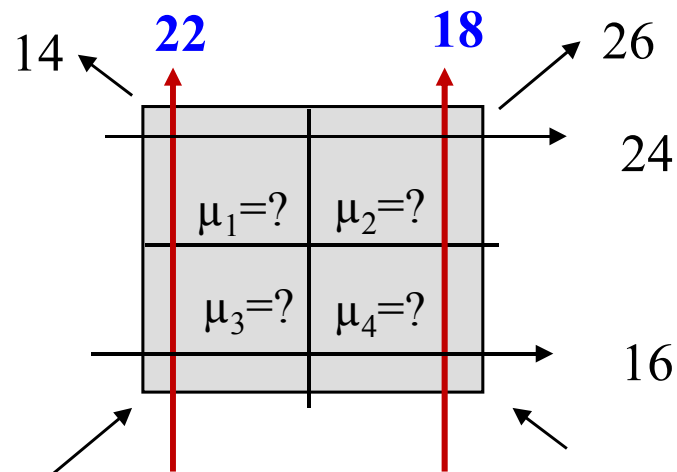
Suppose we are imaging a body slice that consists of four voxels of unit dimension ( $\Delta x=1$ ). The ray sums were measured and are given by the following diagram. Try to determine linear attenuation coefficient of each voxel with algebraic reconstruction technique (ART). Please show each step of iterations.



## Solution:

Recall Algebraic reconstruction technique (ART):

$$\mu_i^{(q+1)} = \mu_i^{(q)} + \frac{p - \sum \mu_i^{(q)}}{N}$$



## Initial iteration, (Vertical), $q=0$

**Initial assumption:**  $\mu_1^{(0)} = \mu_2^{(0)} = \mu_3^{(0)} = \mu_4^{(0)} = 0$

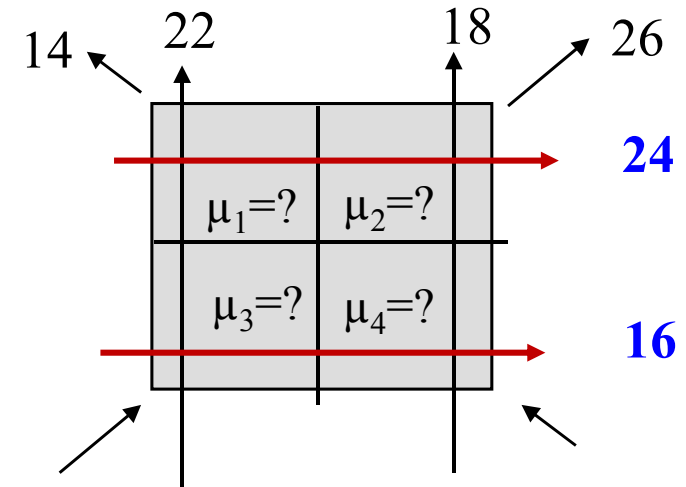
$$p = 22 \Rightarrow \mu_1^{(1)} = \mu_1^{(0)} + \frac{p - [\mu_1^{(0)} + \mu_3^{(0)}]}{2} = 0 + \frac{22 - [0 + 0]}{2} = 11$$

$$p = 18 \Rightarrow \mu_2^{(1)} = \mu_2^{(0)} + \frac{p - [\mu_2^{(0)} + \mu_4^{(0)}]}{2} = 0 + \frac{18 - [0 + 0]}{2} = 9$$

$$p = 22 \Rightarrow \mu_3^{(1)} = \mu_3^{(0)} + \frac{p - [\mu_1^{(0)} + \mu_3^{(0)}]}{2} = 0 + \frac{22 - [0 + 0]}{2} = 11$$

$$p = 18 \Rightarrow \mu_4^{(1)} = \mu_4^{(0)} + \frac{p - [\mu_2^{(0)} + \mu_4^{(0)}]}{2} = 0 + \frac{18 - [0 + 0]}{2} = 9$$

$$\mu_i^{(q+1)} = \mu_i^{(q)} + \frac{p - \sum \mu_i^{(q)}}{N}$$



**Try again, (Horizontal),  $q=1$**

**From initial iteration:**  $\mu_1^{(1)} = 11$ ;  $\mu_2^{(1)} = 9$ ;  $\mu_3^{(1)} = 11$ ;  $\mu_4^{(1)} = 9$

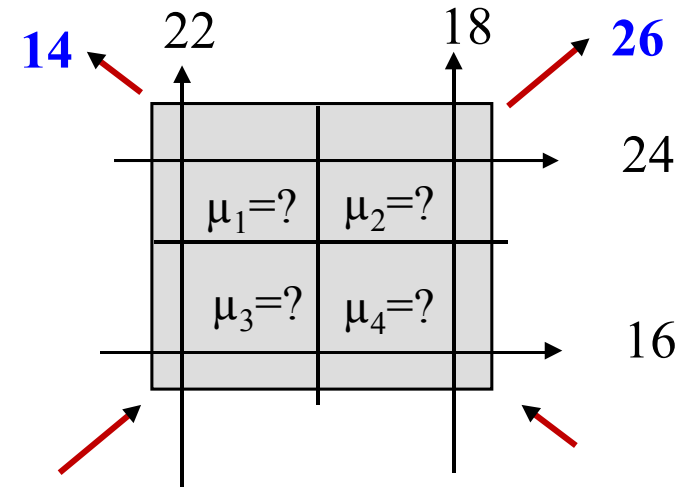
$$p = 24 \Rightarrow \mu_1^{(2)} = \mu_1^{(1)} + \frac{p - [\mu_1^{(1)} + \mu_2^{(1)}]}{2} = 11 + \frac{24 - [11 + 9]}{2} = 13$$

$$p = 24 \Rightarrow \mu_2^{(2)} = \mu_2^{(1)} + \frac{p - [\mu_1^{(1)} + \mu_2^{(1)}]}{2} = 9 + \frac{24 - [11 + 9]}{2} = 11$$

$$p = 16 \Rightarrow \mu_3^{(2)} = \mu_3^{(1)} + \frac{p - [\mu_3^{(1)} + \mu_4^{(1)}]}{2} = 11 + \frac{16 - [11 + 9]}{2} = 9$$

$$p = 16 \Rightarrow \mu_4^{(2)} = \mu_4^{(1)} + \frac{p - [\mu_3^{(1)} + \mu_4^{(1)}]}{2} = 9 + \frac{16 - [11 + 9]}{2} = 7$$

$$\mu_i^{(q+1)} = \mu_i^{(q)} + \frac{p - \sum \mu_i^{(q)}}{N}$$



**Try one more time, (Diagonal),  $q=2$**

**From try again:**  $\mu_1^{(2)} = 13$ ;  $\mu_2^{(2)} = 11$ ;  $\mu_3^{(2)} = 9$ ;  $\mu_4^{(2)} = 7$

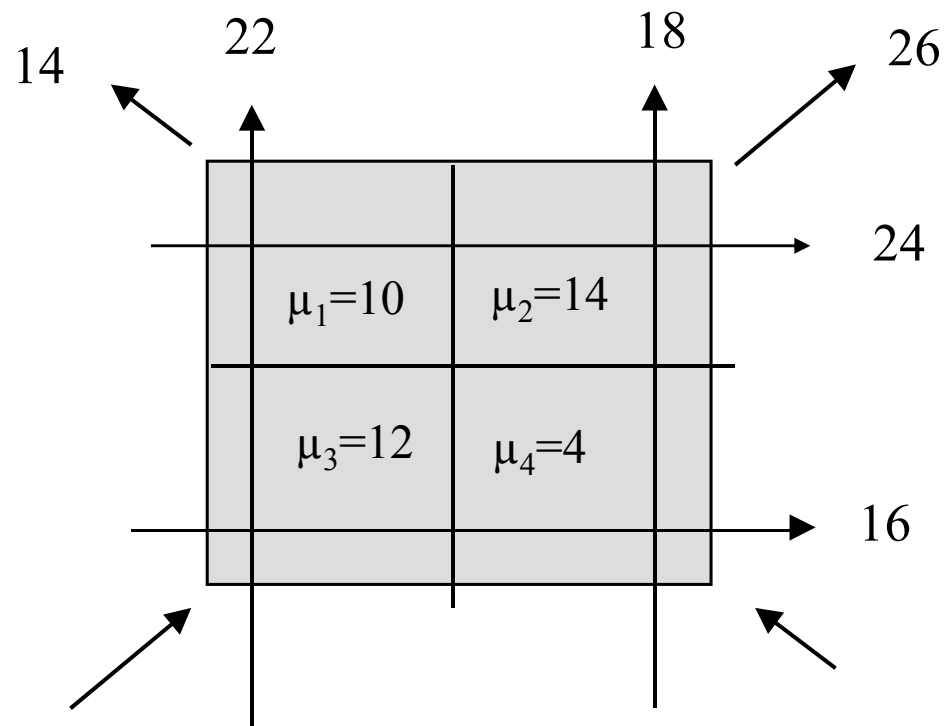
$$p = 14 \Rightarrow \mu_1^{(3)} = \mu_1^{(2)} + \frac{p - [\mu_1^{(2)} + \mu_4^{(2)}]}{2} = 13 + \frac{14 - [13 + 7]}{2} = 10$$

$$p = 26 \Rightarrow \mu_2^{(3)} = \mu_2^{(2)} + \frac{p - [\mu_2^{(2)} + \mu_3^{(2)}]}{2} = 11 + \frac{26 - [11 + 9]}{2} = 14$$

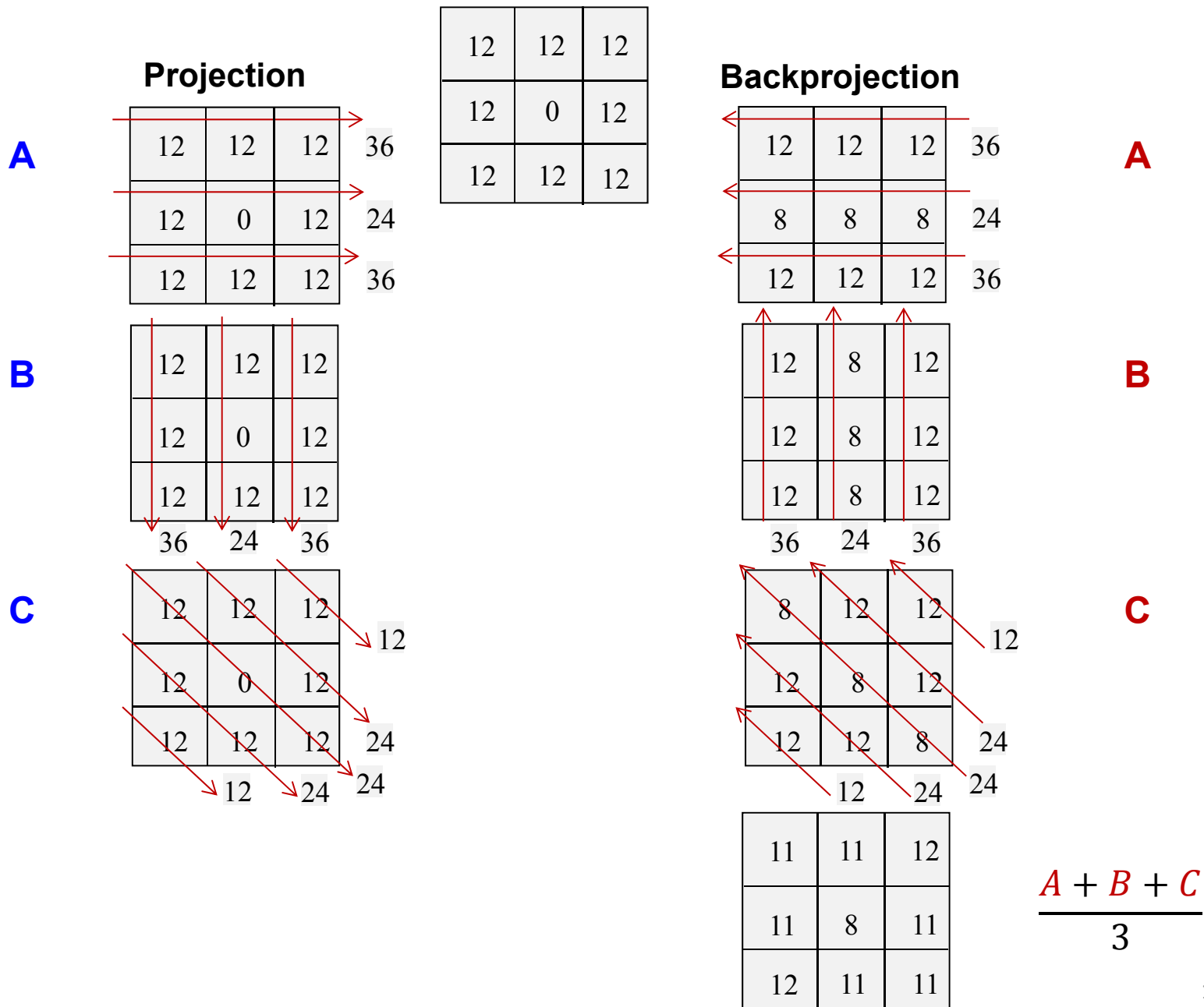
$$p = 26 \Rightarrow \mu_3^{(3)} = \mu_3^{(2)} + \frac{p - [\mu_2^{(2)} + \mu_3^{(2)}]}{2} = 9 + \frac{26 - [11 + 9]}{2} = 12$$

$$p = 14 \Rightarrow \mu_4^{(3)} = \mu_4^{(2)} + \frac{p - [\mu_1^{(2)} + \mu_4^{(2)}]}{2} = 7 + \frac{14 - [13 + 7]}{2} = 4$$

Therefore, we have:  $\mu_1=10$ ;  $\mu_2=14$ ;  $\mu_3=12$ ;  $\mu_4=4$

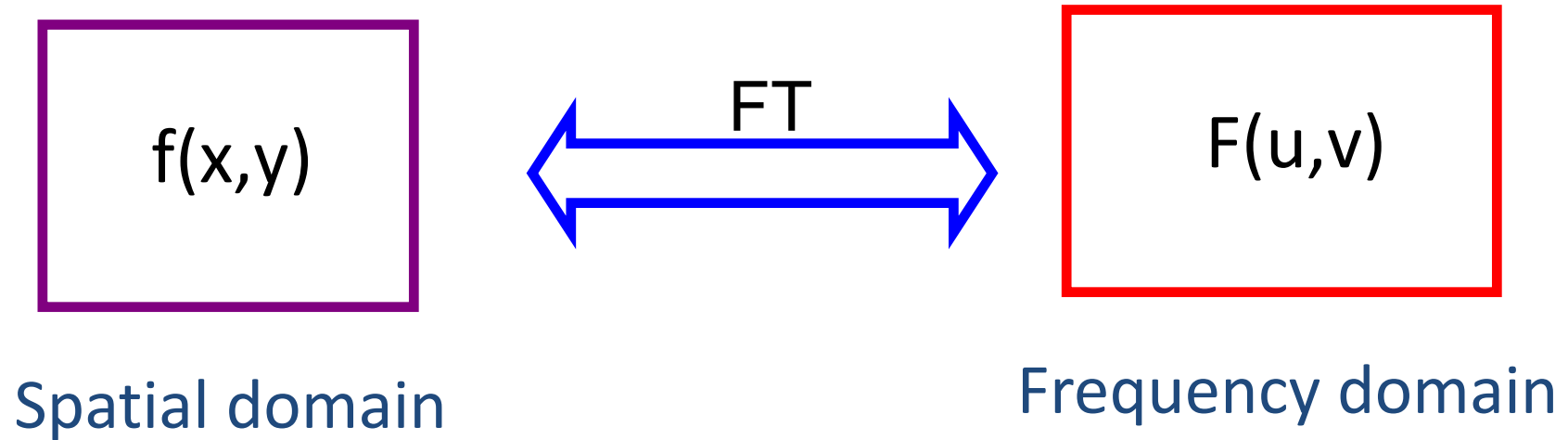


## (c) Backprojection— Conceptual description



#### (4) Reconstruction technique: Fourier transform approach

##### (a) Fourier transformation



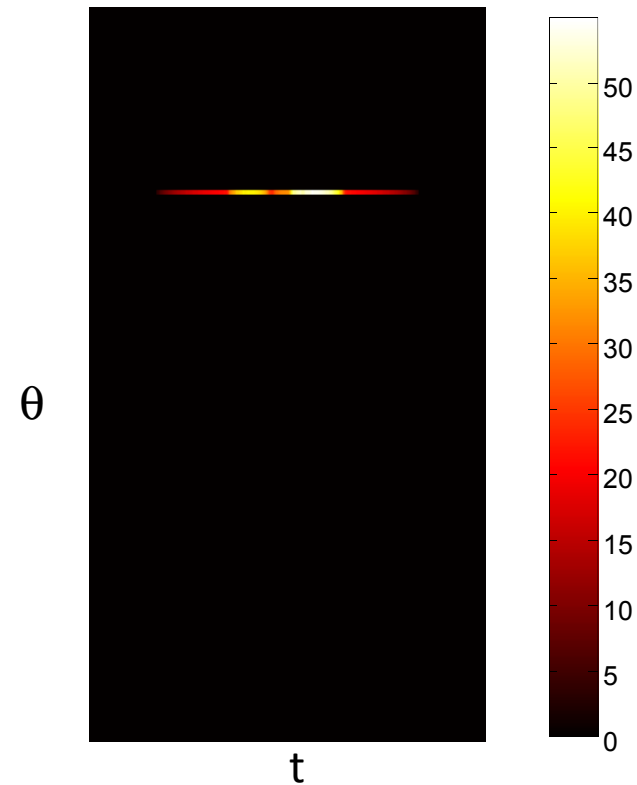
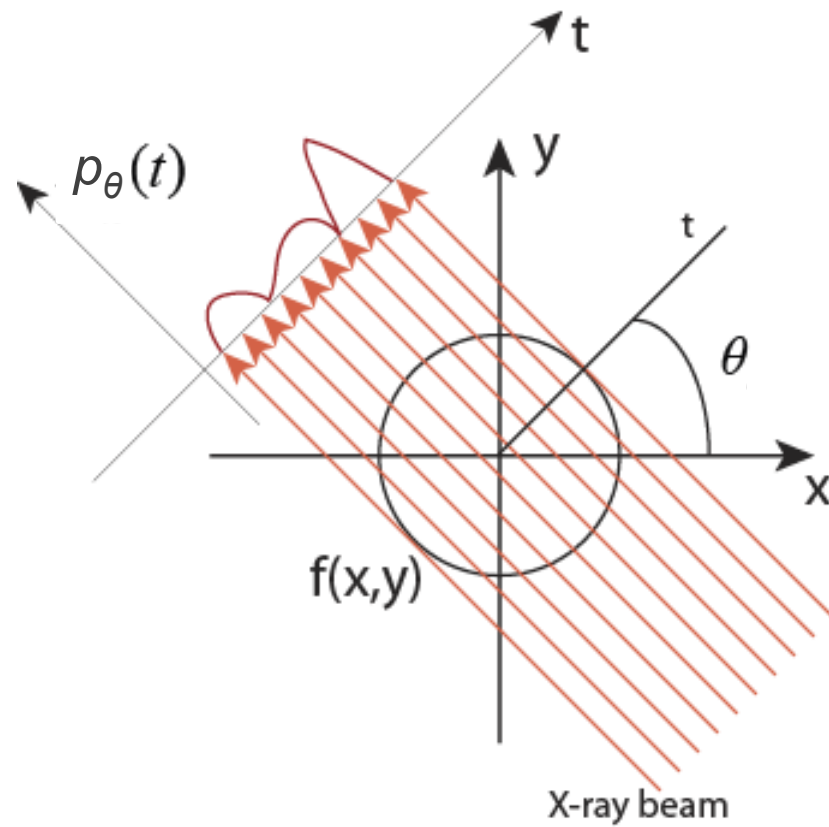
Fourier transform

$$F(u, v) = FT[f(x, y)] = \int_{-\infty}^{\infty} \int_{-\infty}^{\infty} f(x, y) e^{-j2\pi(ux+vy)} dx dy$$

$$f(x, y) = FT^{-1}[F(u, v)] = \int_{-\infty}^{\infty} \int_{-\infty}^{\infty} F(u, v) e^{j2\pi(ux+vy)} du dv$$

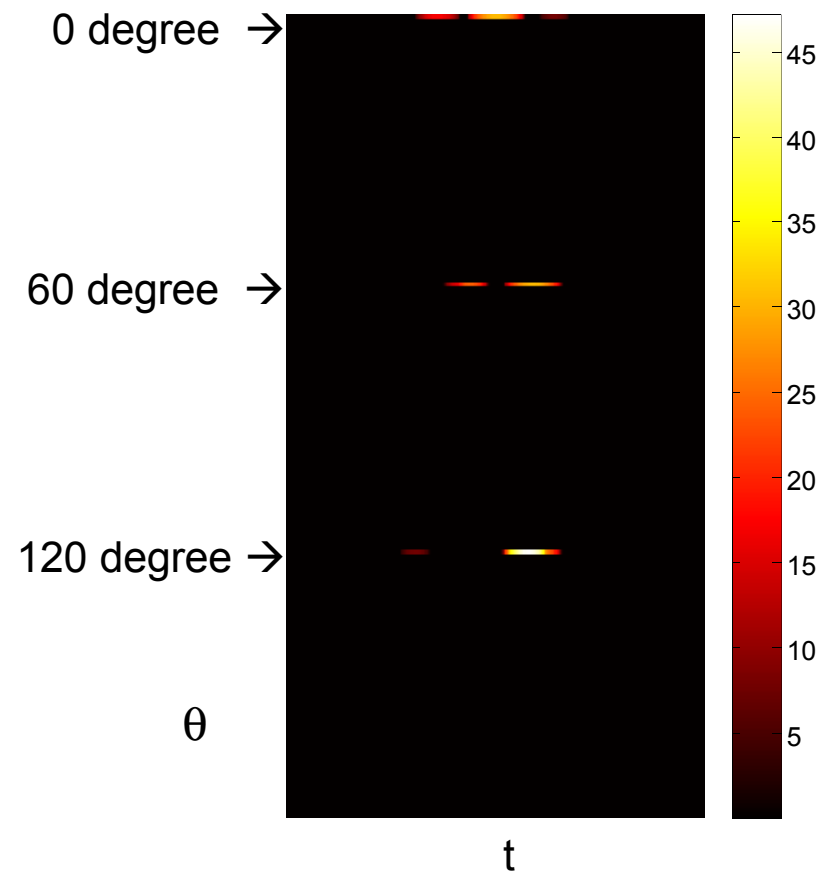
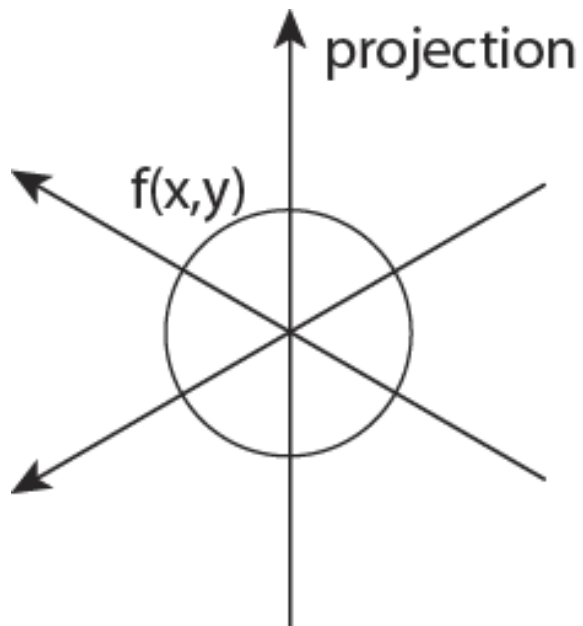


## (b) From projection to sinogram



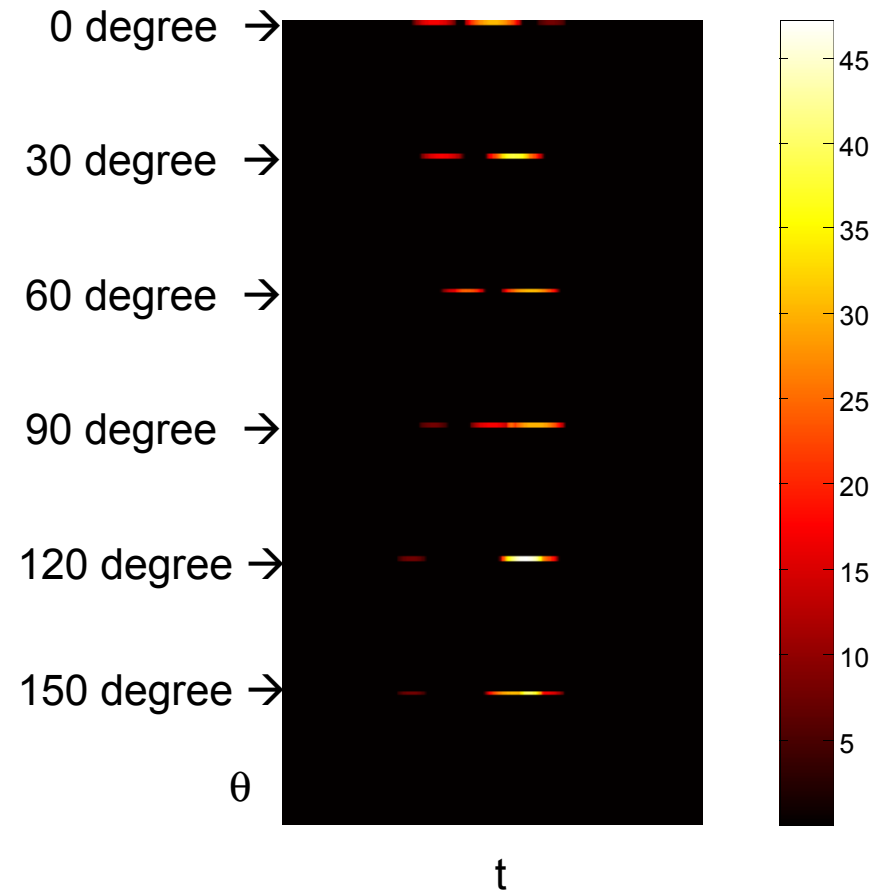
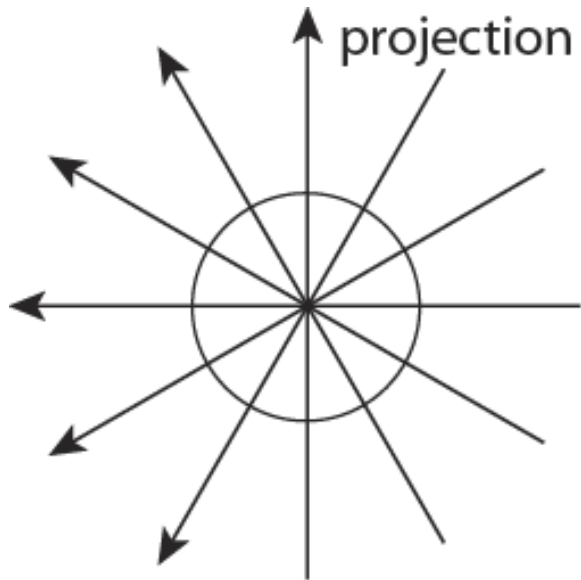
One projection results one “line image”, color bar (right figure) represents intensity variation

## 3 projections at 0, 60, 120 degrees



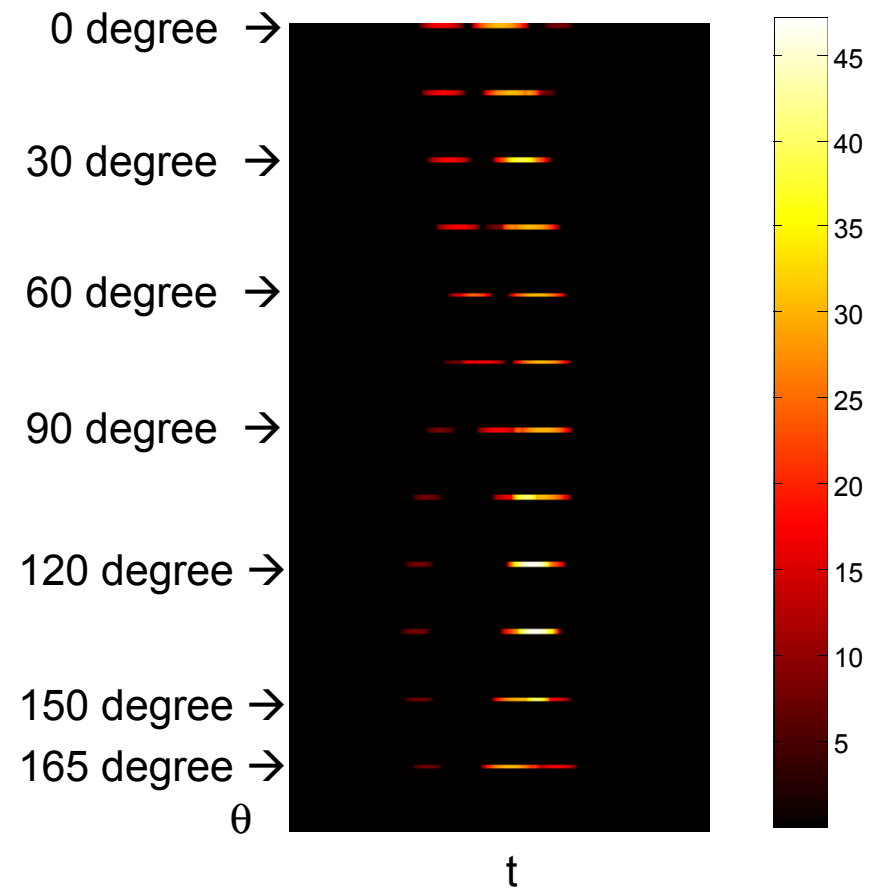
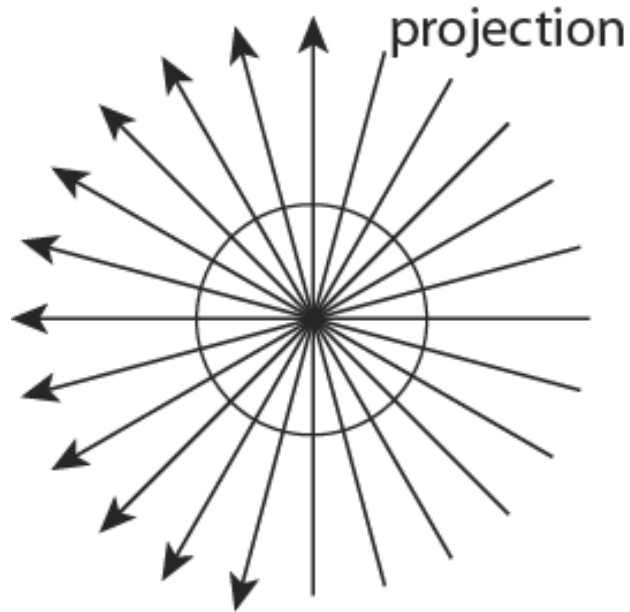
Three projections result 3 “line images”, color bar represents intensity variation

## 6 projections at 0, 30, 60, 90, 120, 150 degree



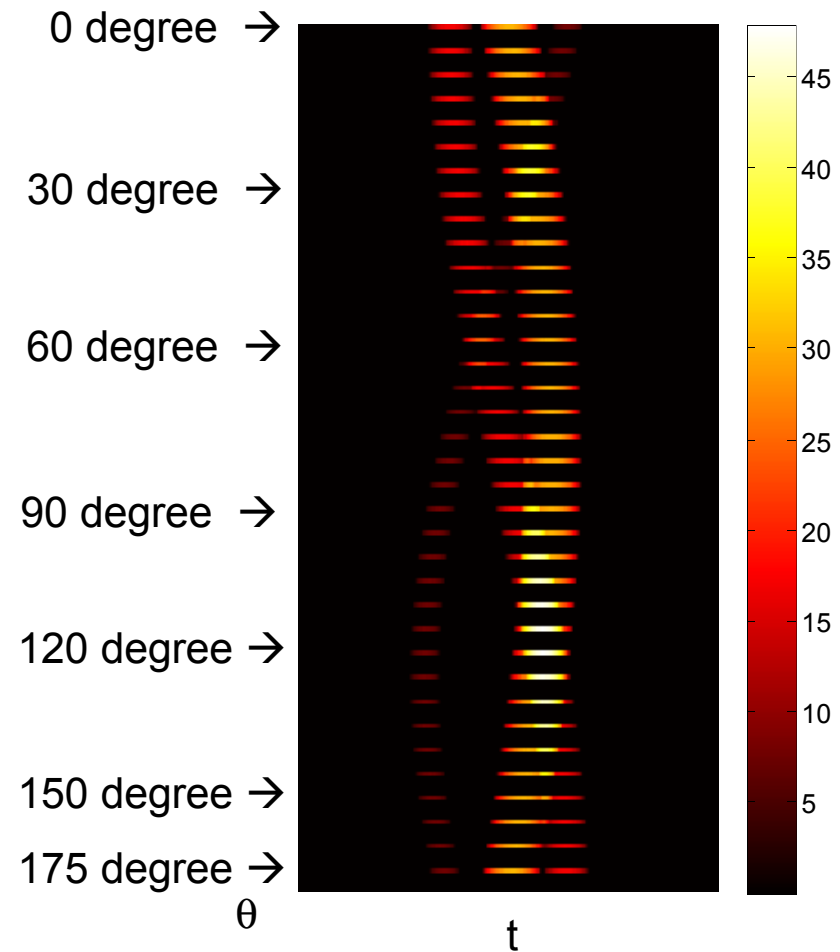
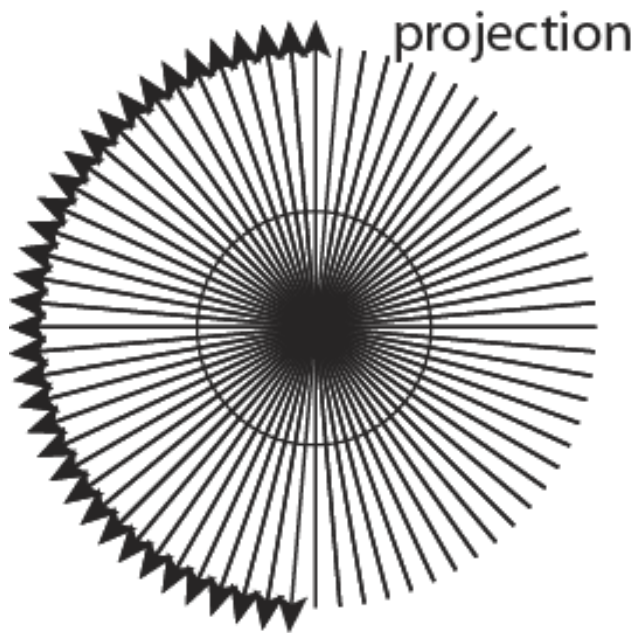
6 “line images” of CT projection obtained at 0, 30, 60, 90, 120, and 150 degree,

## 12 projections at 15 degree increment



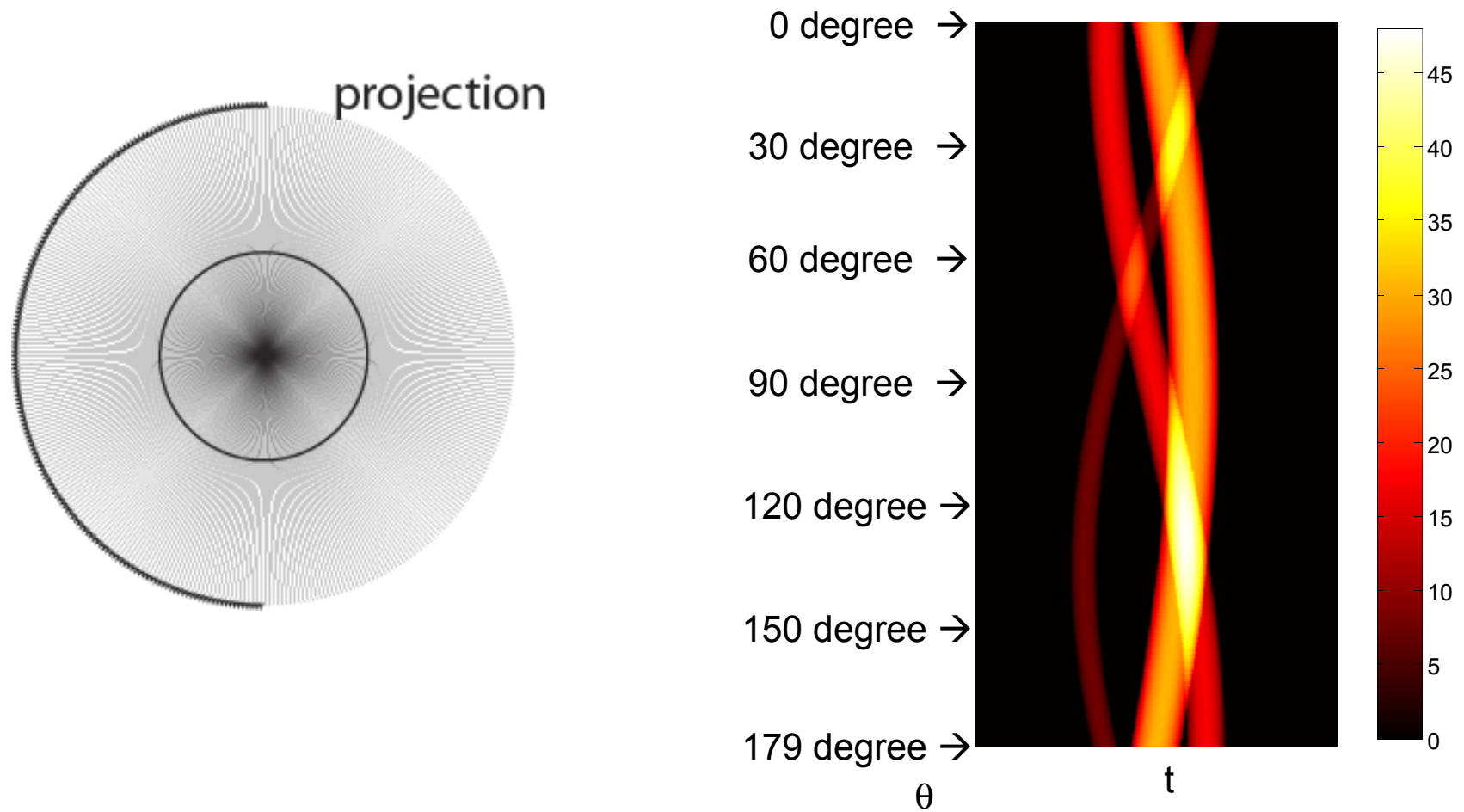
12 “line images” of CT projection obtained at 0, 15, 30, 45, 60, 75, 90, 105, 120, 135, 150, and 165 degree

## A Sinogram obtained from 36 projections at 5 degree increment



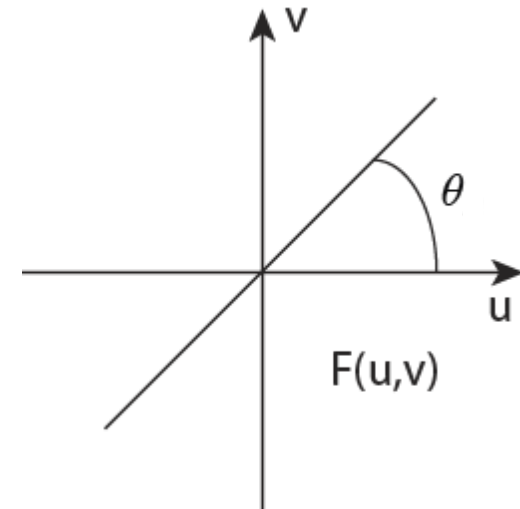
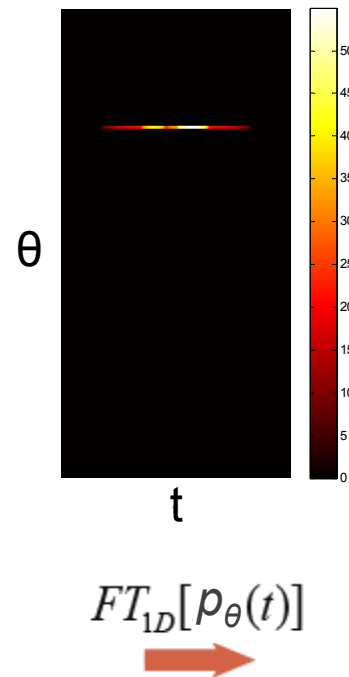
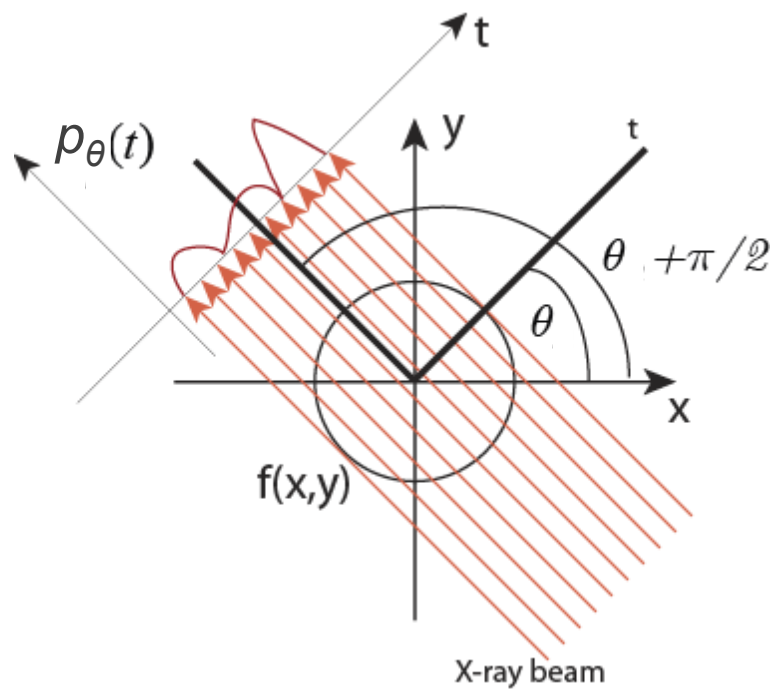
36 "line images" of CT projection obtained at 5 degree increment

## A Sinogram obtained from 180 projections at 1 degree increment



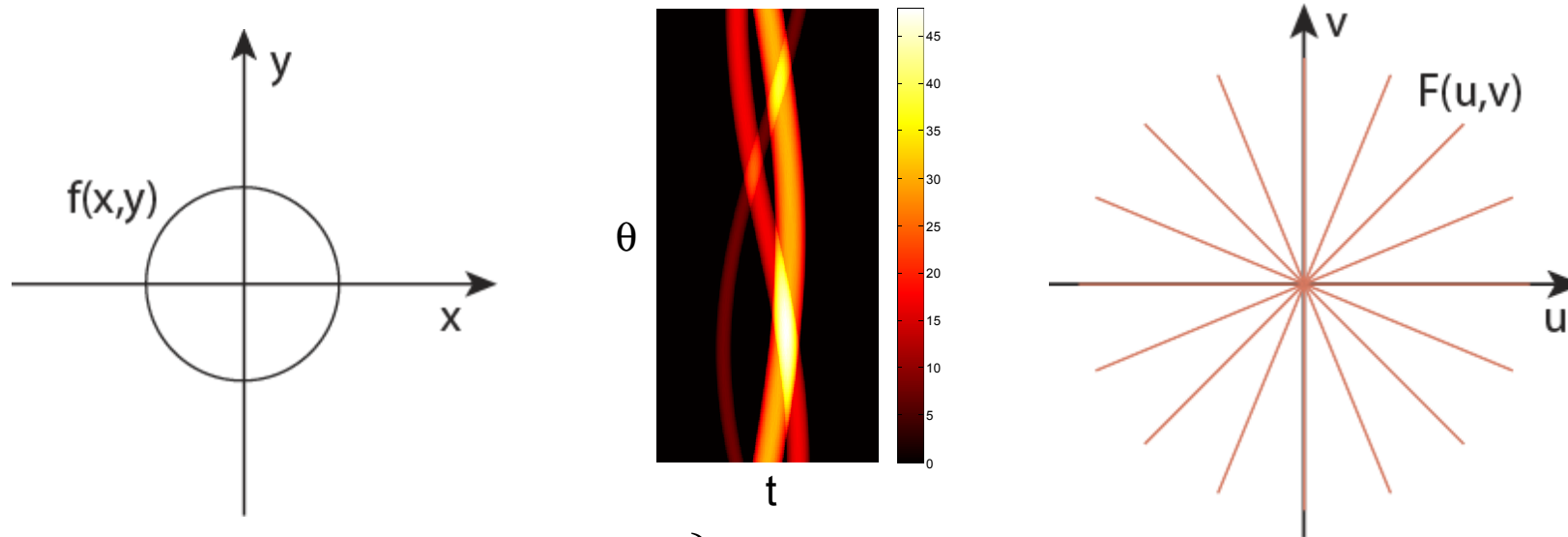
180 "line images" of CT projections formed a Sinogram

## (c) Fourier slice theorem



**Fourier slice theorem:** The Fourier transform of a projection along the line at an angle  $\theta + \pi/2$  with respect to  $x$  axis (left figure) corresponds to the radial line at an angle  $\theta$  with respect to  $u$  axis (right figure).

## Back projections to reconstruct image



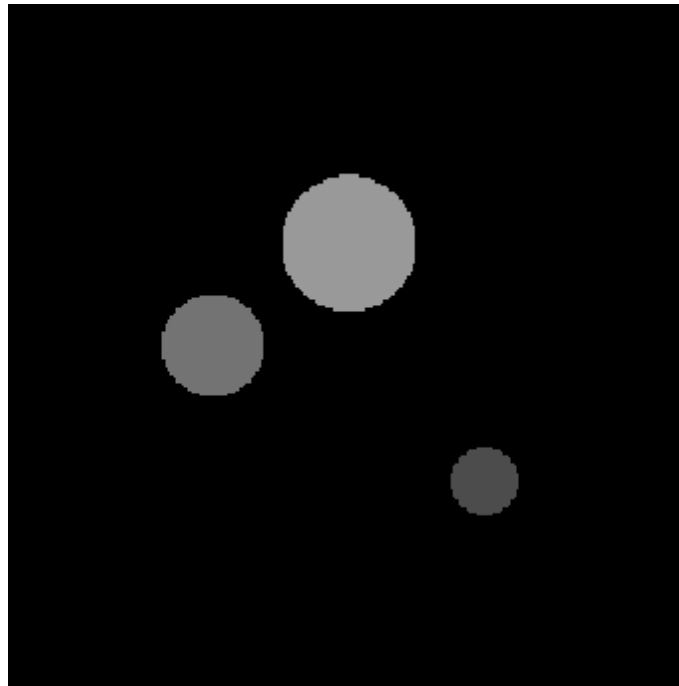
$$\left. \begin{matrix} p_{\theta_1}(t) \\ p_{\theta_2}(t) \\ p_{\theta_3}(t) \\ \dots \\ p_{\theta_n}(t) \end{matrix} \right\} \Rightarrow \sum_{\theta=\theta_1}^{\theta_n} FT_{1D}[p_\theta(t)] \Rightarrow F(u,v)$$

$$\xrightarrow{FT_{2D}^{-1}[F(u,v)]}$$

$$f(x,y) = \int_{-\infty}^{\infty} \int_{-\infty}^{\infty} F(u,v) e^{j2\pi(ux+vy)} du dv$$

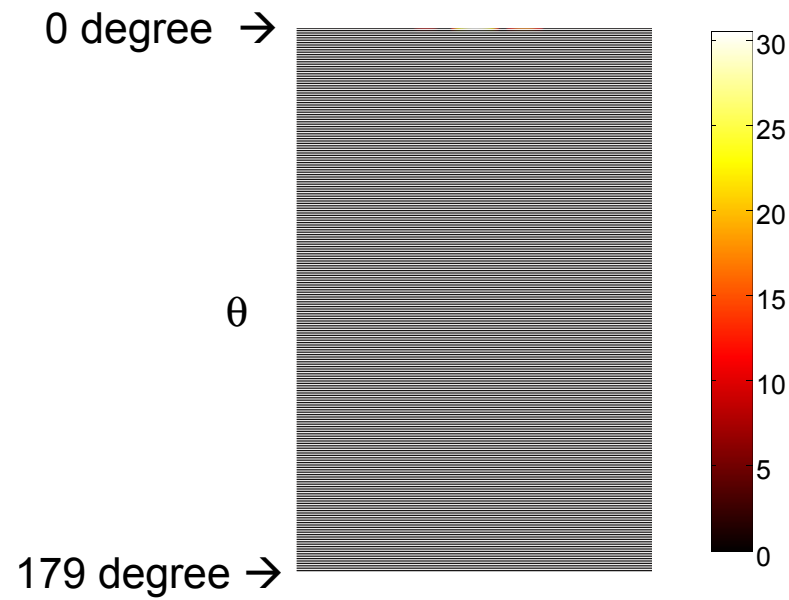


**Example:** Impact of the number of projections

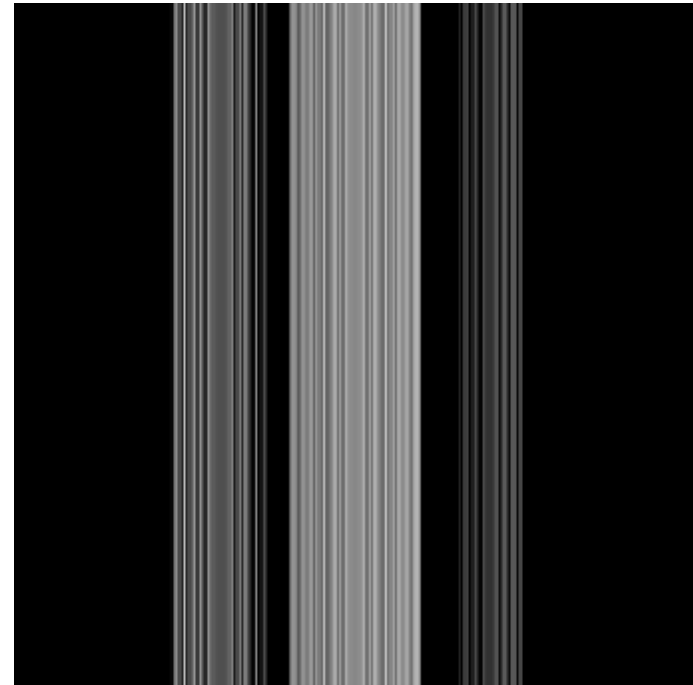


The cross-section of a slice with 3 holes

## 1 projection at 0 degree

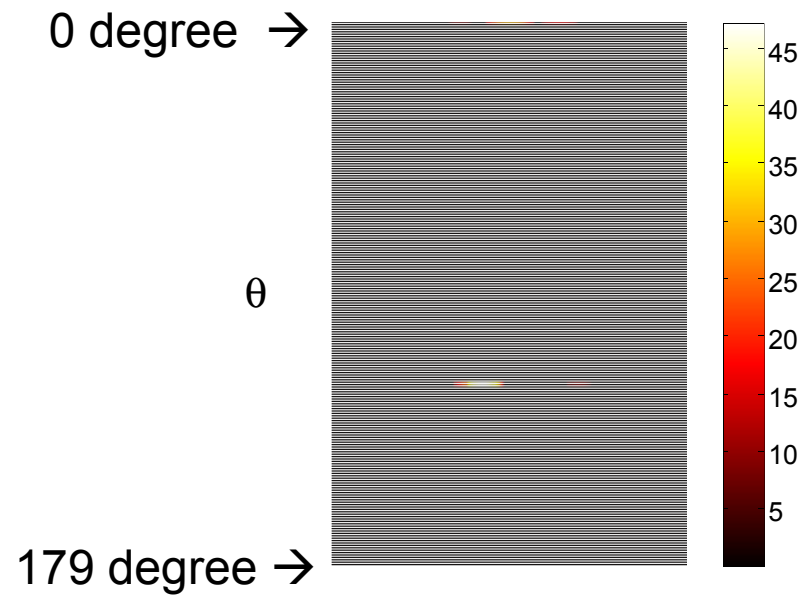


Sinogram

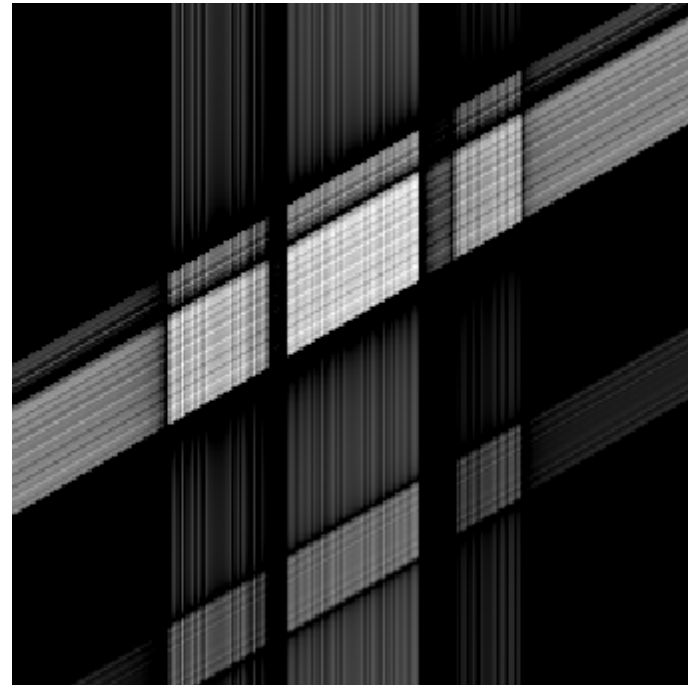


Reconstructed image

## 2 projections at 0, 120 degree

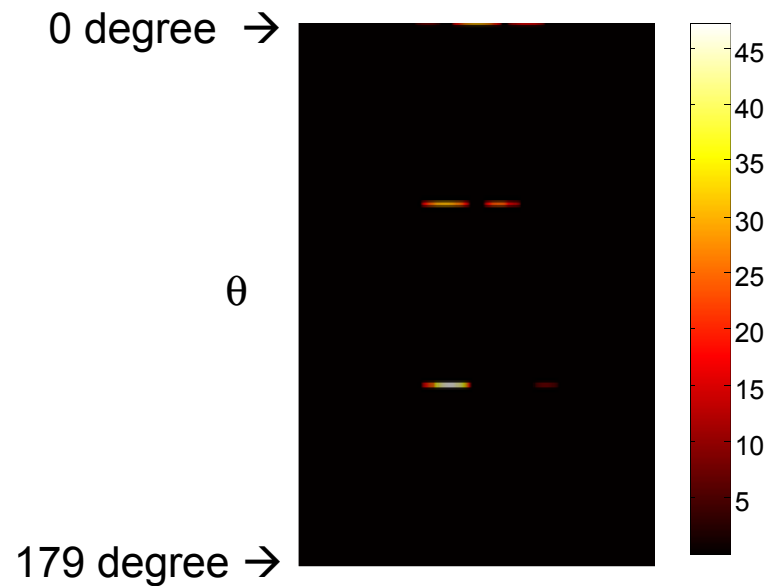


Sinogram

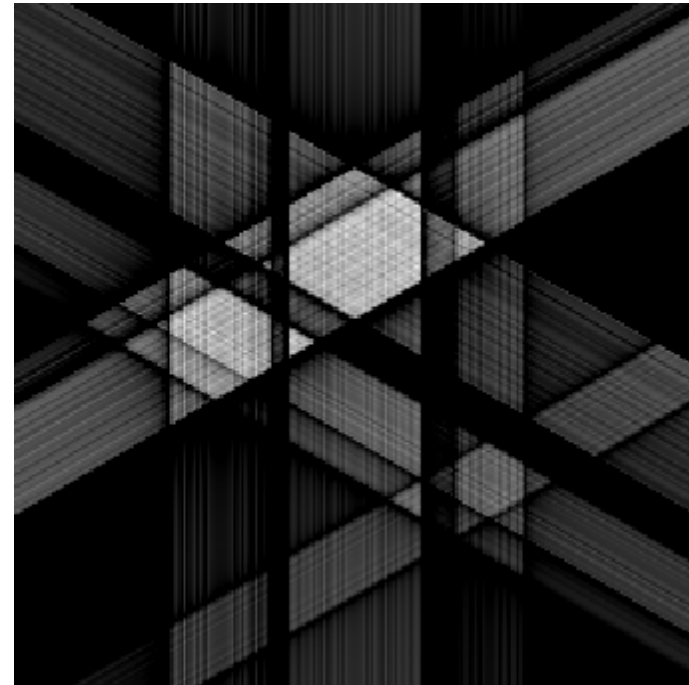


Reconstructed image

## 3 projections at 0, 60, 120 degree

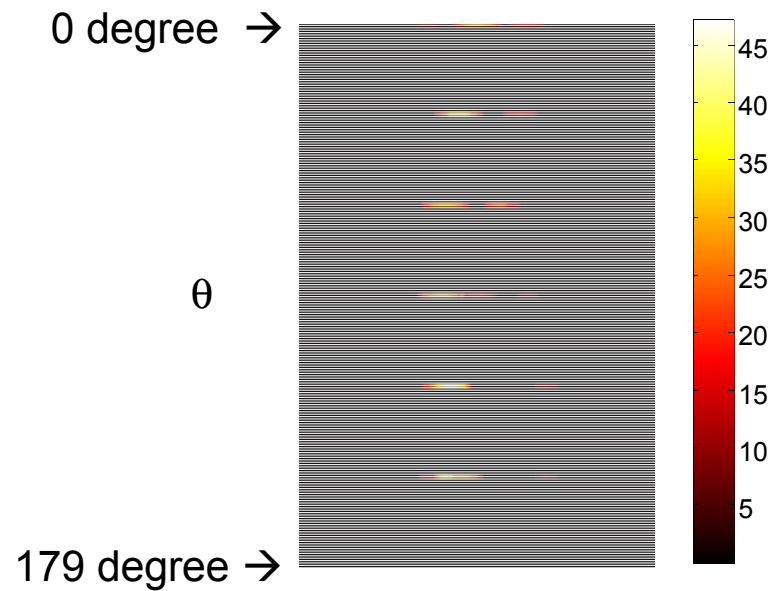


Sinogram

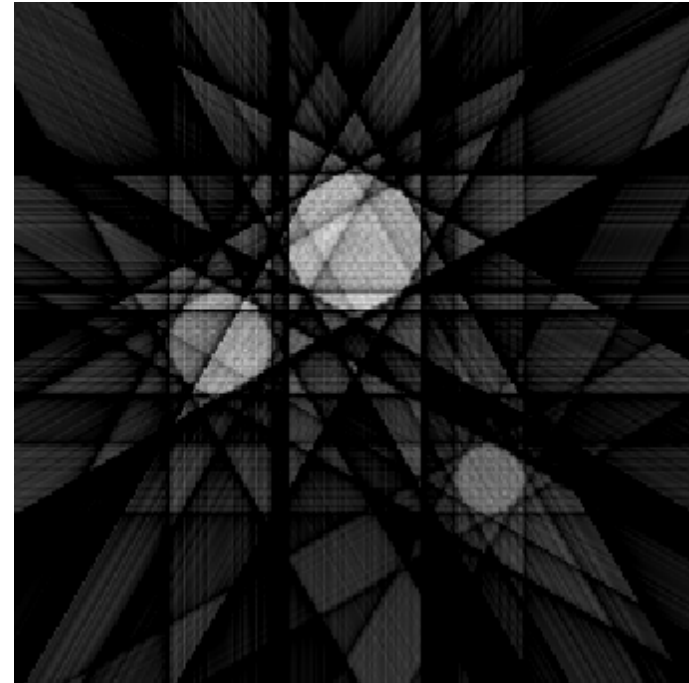


Reconstructed image

6 projections at 0, 30, 60, 90, 120, 150 degree

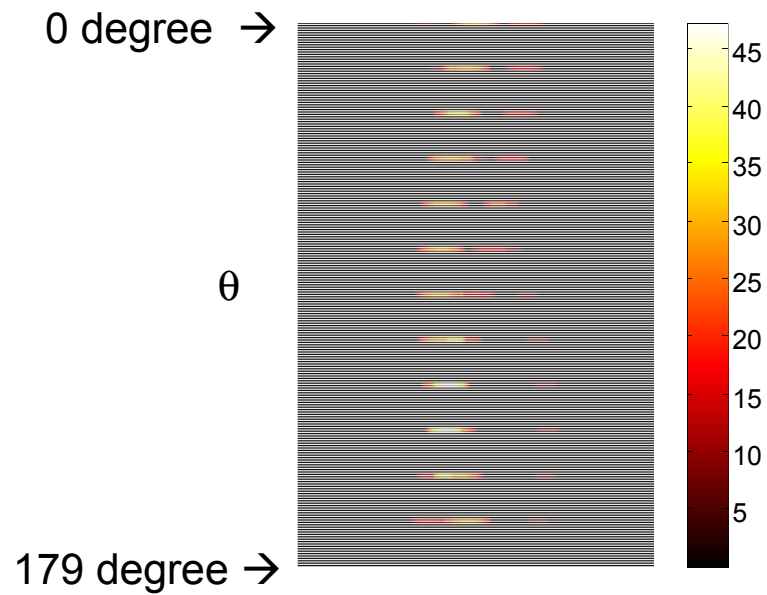


Sinogram

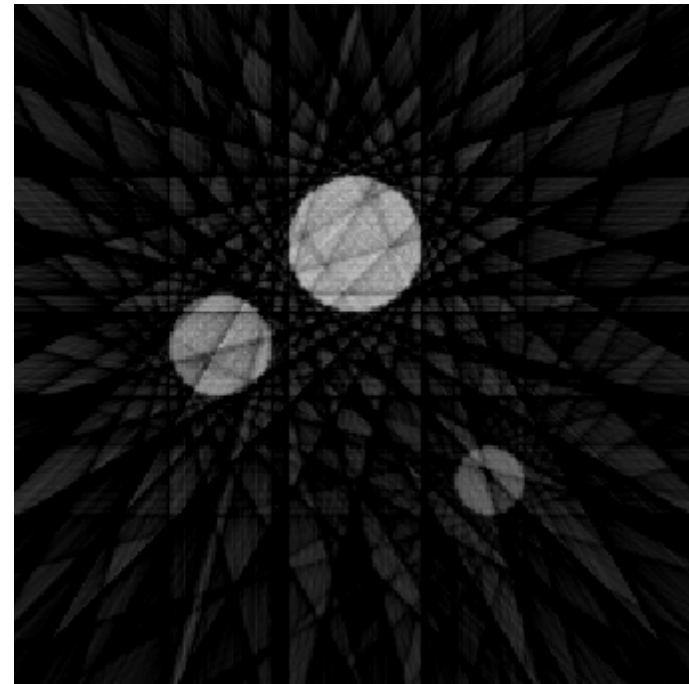


Reconstructed image

## 12 projections at 15 degree increment

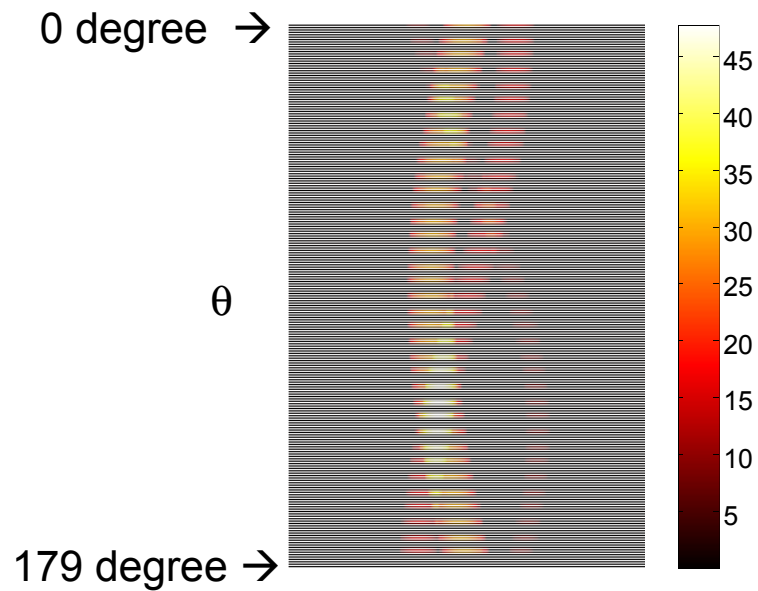


Sinogram

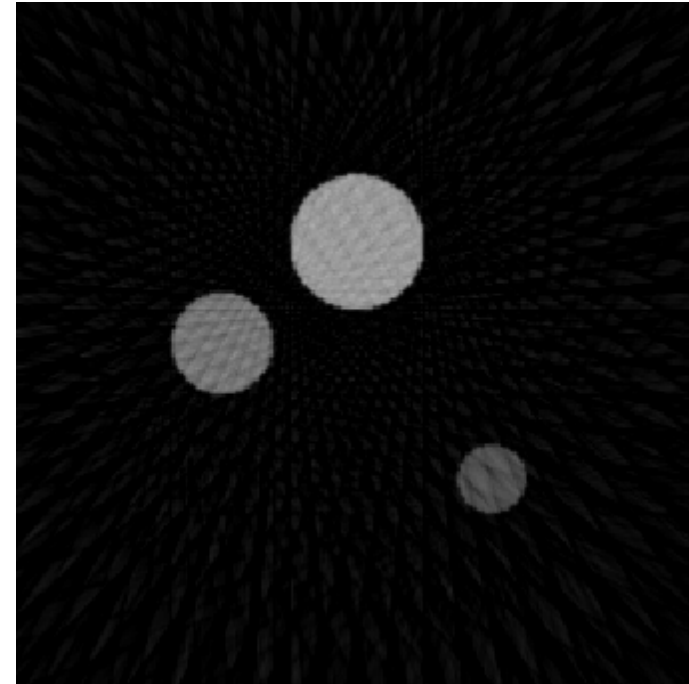


Reconstructed image

## 36 projections at 5 degree increment

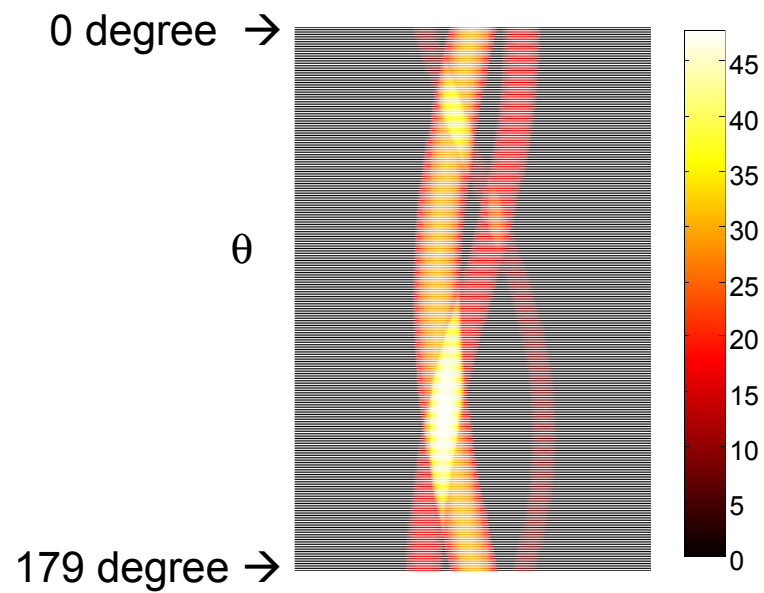


Sinogram

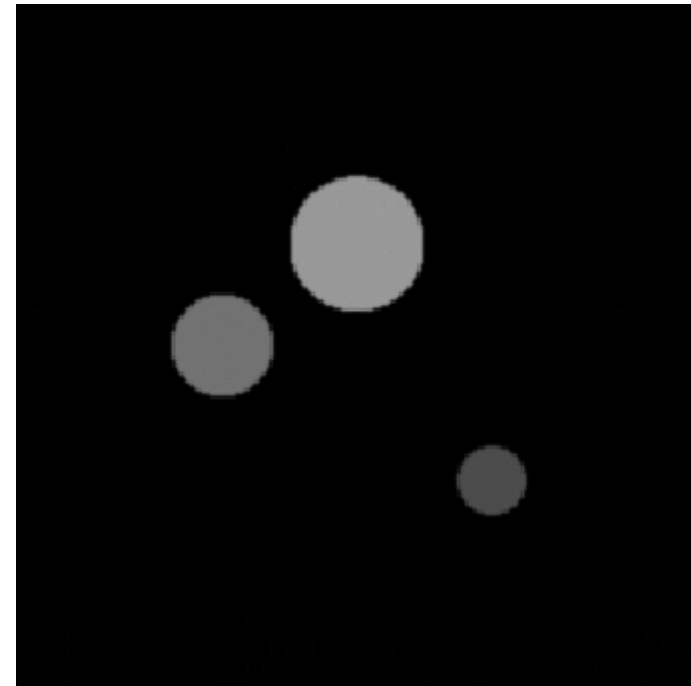


Reconstructed image

180 projections at 1 degree increment (0~179 degree)



Sinogram



Reconstructed image



## (d) Summary of back projection and reconstruction process: Fourier transform approach

### Radon transform

- ❖ Scan the object  $f(x,y)$ , to obtain projections at a series of angles. Each projection results a 1D “line of data” at the corresponding angle,  $p_{\theta}(t)$
- ❖ A **2D Sinogram** is obtained by combining all  $p_{\theta_1}(t), p_{\theta_2}(t) \dots$

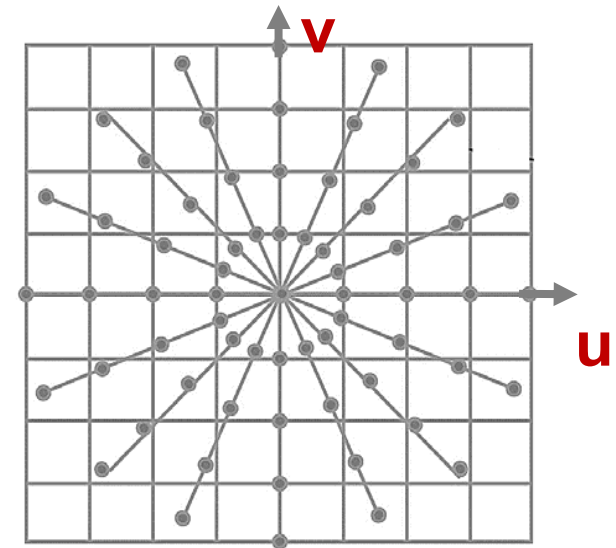
### Inverse Radon transform

- ❖ Apply 1D Fourier transform to each of the projections,  $p_{\theta}(t) \dots$
- ❖ In Fourier space, each of these **1D FT** results a line inclined at the corresponding angle of the projection. All together it is the **2D Fourier transform**,  $F(u,v)$ , of the cross-section of the object,  $f(x,y)$
- ❖ Perform inverse Fourier transform to reconstruct  $f(x,y)$ .

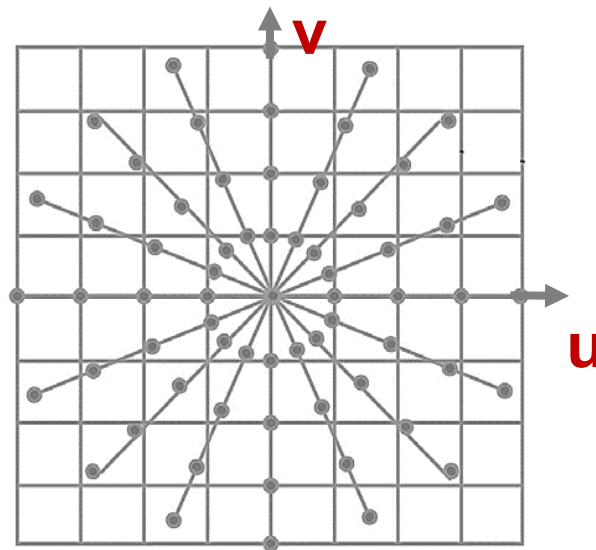
## (5) Filtered backprojection approach

### (a) Limitation of backprojection algorithm

- ❖ The backprojection algorithm discussed earlier provides a straightforward solution for CT reconstruction.
- ❖ It however has some limitations in practical implementation.
- ❖ With backprojection method, each of the **1D *FT*** of the projection results a line inclined at the corresponding angle of that projection on Fourier domain (frequency domain).
- ❖ As shown by the figure here, data from all projections fall on a format of polar coordinate.

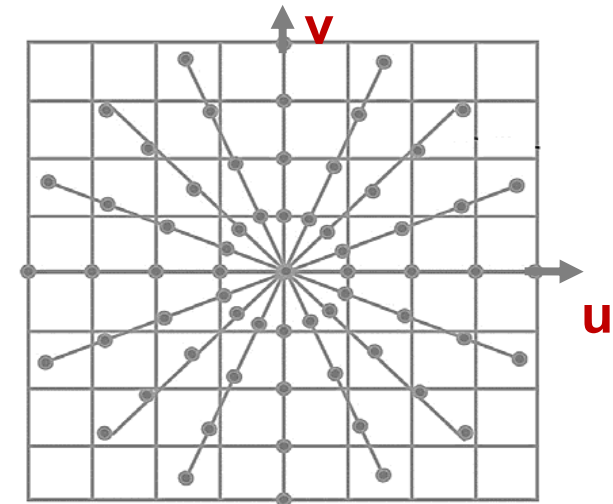


- ❖ The computer implementation of *2D inverse FT*  $f(x, y) = FT^{-1}[F(u, v)]$  uses FFT algorithm. Accordingly, data in polar format have to be interpolated to a Cartesian coordinate.
- ❖ A single error introduced in the interpolation process in the *frequency domain* may affect the appearance of the entire reconstructed image in *spatial domain*.

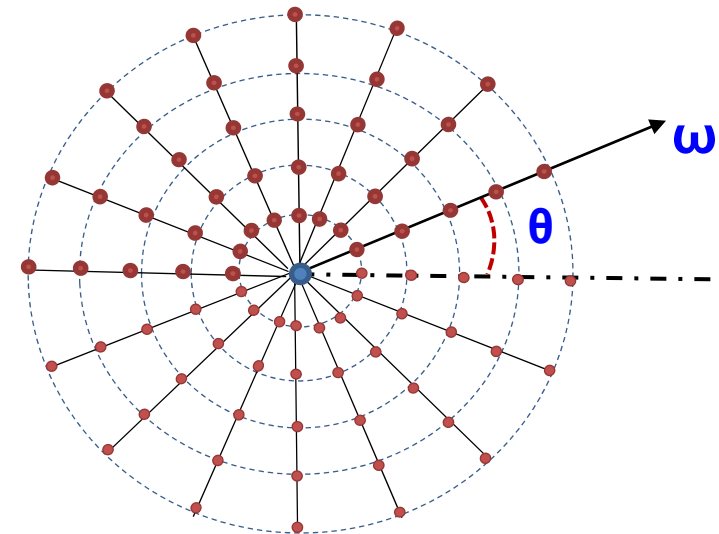


## (b) Conceptual understanding of filtered backprojection

- ❖ How to minimize the impact of these errors, and to improve the quality of the reconstructed images?
- ❖ First, switch from a Cartesian coordinate  $(u, v)$  to a polar coordinate  $(\omega, \theta)$ . The purpose of the coordinate switch is to express the quantity  $F(u, v)$  in the more natural form in which the data are collected.
- ❖ Then conduct derivations to obtain widely used **filtered backprojection algorithm**.



Cartesian coordinate



Polar coordinate

### (c) Derivation of the filtered backprojection formula

From  $F(u, v)$  to  $P(\omega, \theta)$

- ❖ The image function  $f(x, y)$  can be recovered by the inverse Fourier transform of  $F(u, v)$ :

$$f(x, y) = \int_{-\infty}^{\infty} \int_{-\infty}^{\infty} F(u, v) e^{j2\pi(xu + yv)} du dv \quad (1)$$

- ❖ In polar coordinates, the inverse Fourier transform can be written as:

$$f(x, y) = \int_0^{2\pi} \int_0^{\infty} F(\omega \cos \theta, \omega \sin \theta) e^{j2\pi\omega(x \cos \theta + y \sin \theta)} \omega d\omega d\theta \quad (2)$$

**with:**  $u = \omega \cos(\theta), \quad v = \omega \sin(\theta)$

$$du dv = \begin{vmatrix} \frac{\partial u}{\partial \omega} & \frac{\partial u}{\partial \theta} \\ \frac{\partial v}{\partial \omega} & \frac{\partial v}{\partial \theta} \end{vmatrix} d\omega d\theta = \omega d\omega d\theta$$

❖ Let:

$$P(\omega, \theta) = F(\omega \cos(\theta), \omega \sin(\theta))$$

❖ We can rewrite Eq. (2) as:

$$\begin{aligned} f(x, y) &= \int_0^{2\pi} \int_0^{\infty} P(\omega, \theta) e^{j2\pi\omega(x \cos \theta + y \sin \theta)} \omega d\omega d\theta \\ &= \int_0^{2\pi} d\theta \int_0^{\infty} P(\omega, \theta) e^{j2\pi\omega(x \cos \theta + y \sin \theta)} \omega d\omega \\ &= \int_0^{\pi} d\theta \int_0^{\infty} P(\omega, \theta) e^{j2\pi\omega(x \cos \theta + y \sin \theta)} \omega d\omega \\ &\quad + \int_{\pi}^{2\pi} d\theta \int_0^{\infty} P(\omega, \theta) e^{j2\pi\omega(x \cos \theta + y \sin \theta)} \omega d\omega \end{aligned} \tag{3}$$

**Continue from Eq. (3):**

$$\begin{aligned} f(x, y) &= \int_0^{\pi} d\theta \int_0^{\infty} P(\omega, \theta) e^{j2\pi\omega(x \cos \theta + y \sin \theta)} \omega d\omega \\ &\quad + \int_0^{\pi} d\theta \int_0^{\infty} P(\omega, \theta + \pi) e^{j2\pi\omega[x \cos(\theta + \pi) + y \sin(\theta + \pi)]} \omega d\omega \\ &= \int_0^{\pi} d\theta \int_0^{\infty} P(\omega, \theta) e^{j2\pi\omega(x \cos \theta + y \sin \theta)} \omega d\omega \\ &\quad + \int_0^{\pi} d\theta \int_0^{\infty} P(\omega, \theta + \pi) e^{-j2\pi\omega(x \cos(\theta) + y \sin \theta)} \omega d\omega \end{aligned} \quad (4)$$

**Note:**  $\cos(\theta + \pi) = -\cos \theta$   
 $\sin(\theta + \pi) = -\sin \theta$

- ❖ The  $f(x,y)$  is a real function, its Fourier transform has the following **symmetry property** in the frequency domain:

$$P(\omega, \theta + \pi) = P(-\omega, \theta) \quad (5)$$

- ❖ Accordingly Eq (4) becomes:

$$\begin{aligned} f(x, y) &= \int_0^{\pi} d\theta \int_0^{\infty} P(\omega, \theta) e^{j2\pi\omega(x \cos \theta + y \sin \theta)} \omega d\omega \\ &\quad + \int_0^{\pi} d\theta \int_0^{\infty} P(-\omega, \theta) e^{-j2\pi\omega(x \cos \theta + y \sin \theta)} \omega d\omega \\ &= \int_0^{\pi} d\theta \int_0^{\infty} P(\omega, \theta) e^{j2\pi\omega(x \cos \theta + y \sin \theta)} \omega d\omega \\ &\quad + \int_0^{\pi} d\theta \int_{-\infty}^0 P(\omega, \theta) e^{j2\pi\omega(x \cos(\theta) + y \sin \theta)} |\omega| d\omega \end{aligned} \quad (6)$$



❖ Then:

$$f(x, y) = \int_0^{\pi} \int_{-\infty}^{\infty} P(\omega, \theta) e^{j2\pi\omega[x\cos\theta + y\sin\theta]} |\omega| d\omega d\theta \quad (7)$$

❖ Let:

$$t = x \cos(\theta) + y \sin(\theta)$$

❖ Then Eq. (7) can be rewritten as

$$f(x, y) = \int_0^{\pi} \left[ \int_{-\infty}^{\infty} P(\omega, \theta) \times |\omega| \times e^{j2\pi\omega t} d\omega \right] d\theta \quad (8)$$

❖ In Eq. (8), the  $P(\omega, \theta)$  is the *1D FT* of the measured parallel projection  $p_{\theta}(t)$  *at angle  $\theta$* .

**Note:**  $p_{\theta}(t)$  is in spatial domain

### (d) The filtered backprojection and the ramp filter

❖ In the spatial domain, let  $h(t)$  as the inverse *1D FT* of  $|\omega|$

$$h(t) = FT^{-1}(|\omega|) = \int_{-\infty}^{\infty} |\omega| e^{j2\pi\omega t} d\omega \quad (9)$$

❖ Recall Eq. (8)

$$f(x, y) = \int_0^{\pi} \left[ \int_{-\infty}^{\infty} P(\omega, \theta) \times |\omega| \times e^{j2\pi\omega t} d\omega \right] d\theta = \int_0^{\pi} [p_{\theta}(t) \otimes h(t)] d\theta \quad (10)$$

where, the projection  $p_{\theta}(t)$  is the inverse *1D FT* of  $P(\omega, \theta)$

❖ In the above equation, the function  $|\omega|$  is a filter function in frequency domain, it is called a **ramp filter**.

- ❖ As an important part of the filtered backprojection algorithm, the **ramp filter**  $|\omega|$  prefers the high frequency contents of the projection over the low frequency contents.
- ❖ In fact, the **ramp filter** reduces the blurring caused by backprojection.

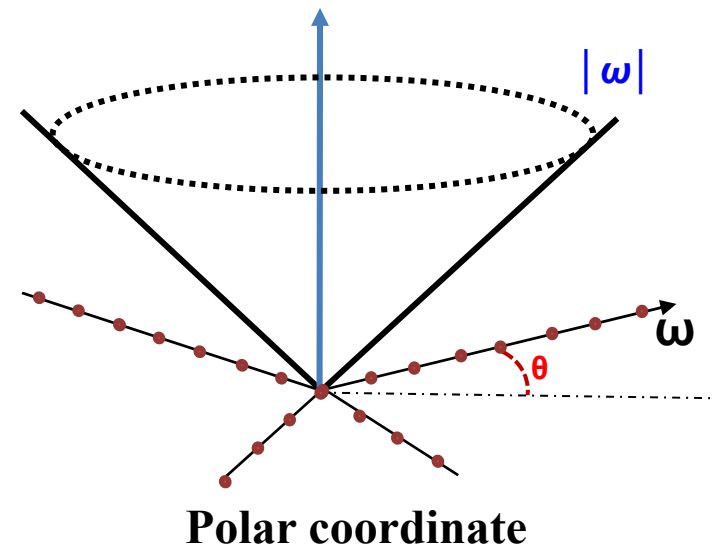
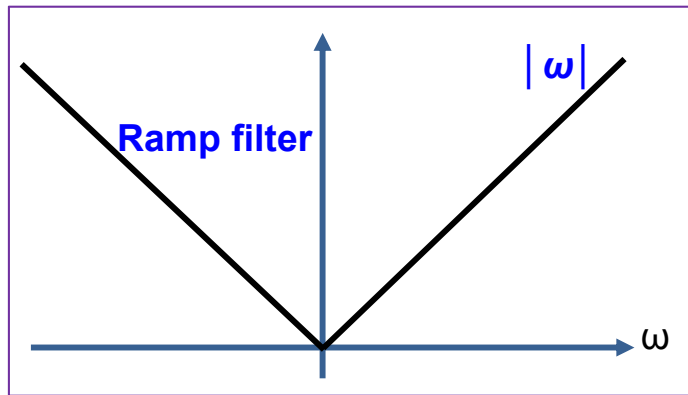
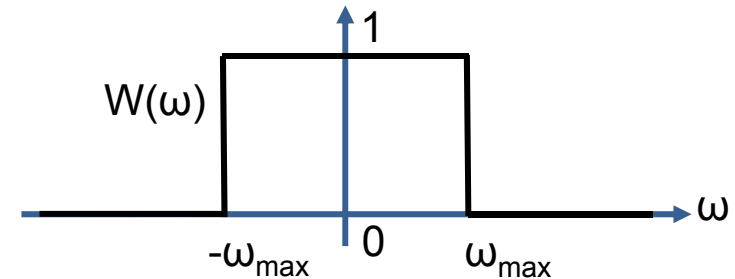


**Fig.** Illustration of the impact of the weighting function (**ramp filter**) in the frequency domain.

### (e) Filtered backprojection and window function

- ❖  $h(t)$  in Eq. (9) cannot be directly determined and calculated over a range between  $(-\infty, \infty)$ .
- ❖ *Assume* that the Fourier transform of the projection is band-limited, over a range of  $[-\omega_{\max}, \omega_{\max}]$  in frequency domain.
- ❖ Let  $W(\omega)$  be a **rectangular** window function, shown by Eq.(11)

$$W(\omega) = \begin{cases} 1 & |\omega| \leq \omega_{\max} \\ 0 & \text{other} \end{cases} \quad (11)$$



- ❖ Based on the **Nyquist sampling theorem**,  $\omega_{\max}$  should equal to  $1/(2\delta)$ , where  $\delta$  is the projection **sampling interval**.

$$\omega_{\max} = \frac{1}{2\delta} \quad (12)$$

- ❖ Under this condition, multiply the original **ramp filter**  $|\omega|$  with **window function**  $W(\omega)$ , Eq. (9) can be expressed as follows in **band-limited form**:

$$h(t) = \int_{-\infty}^{\infty} |\omega| \times W(\omega) \times e^{j2\pi\omega t} d\omega = \int_{-\omega_{\max}}^{\omega_{\max}} |\omega| \times e^{j2\pi\omega t} d\omega \quad (13)$$

- ❖ Finally, Eq.(10) becomes:

$$f(x, y) = \int_0^{\pi} [p_{\theta}(t) \otimes h(t)] d\theta = \int_0^{\pi} \left[ \int_{-\omega_{\max}}^{\omega_{\max}} P(\omega, \theta) \times |\omega| \times e^{j2\pi\omega t} d\omega \right] d\theta \quad (14)$$

- ❖ Here, the  $f(x, y)$  is the reconstructed image by filtered backprojection method with a **band-limited rectangular window** function.

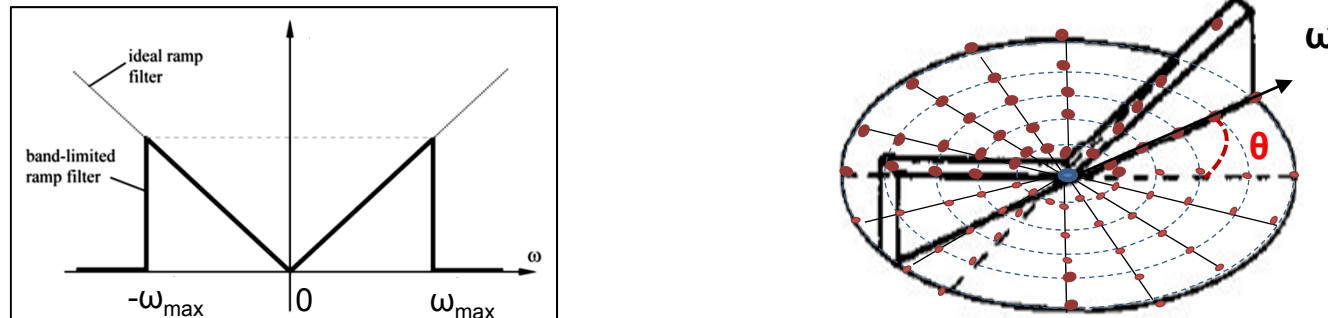


Fig. Frequency representation of the band-limited ramp filter with rectangular window function applied

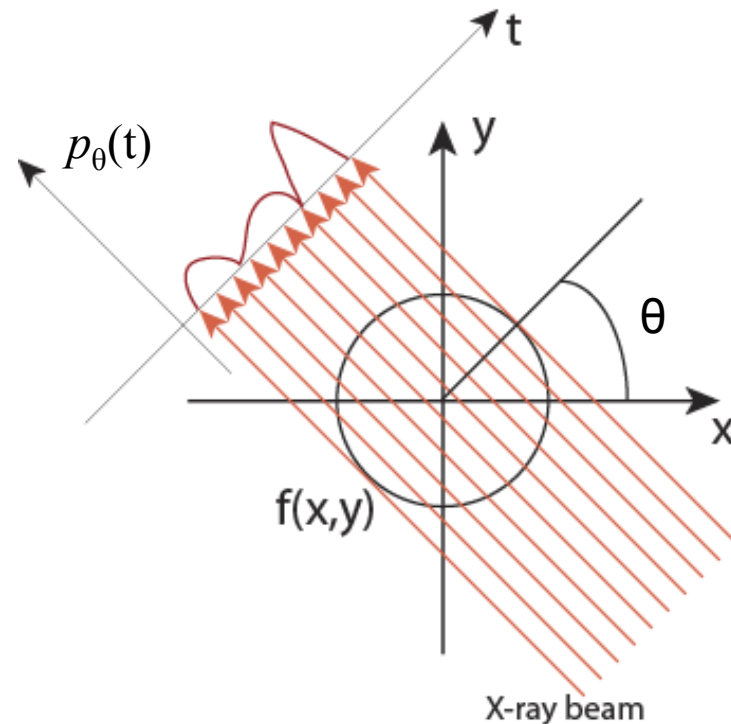
- ❖ In practice, **other filters** can be used in backprojections process.

## Exercise-2:

This problem is related to the CT reconstruction technique (Fourier slice theorem based back projection approach). Assuming that a series of projections from  $0^\circ$  to  $180^\circ$  at  $1^\circ$  increments; resulted a Sinogram that can be expressed as:

$$p_\theta(t) = \sin \theta \times \Lambda(t)$$

Based on Fourier slice theorem, please determine the mathematical expression of the function in Fourier domain at  $\theta=45^\circ$ .



### Solution:

From  $0^0$  to  $180^0$  at  $1^0$  increments, the sinogram can be expressed as:

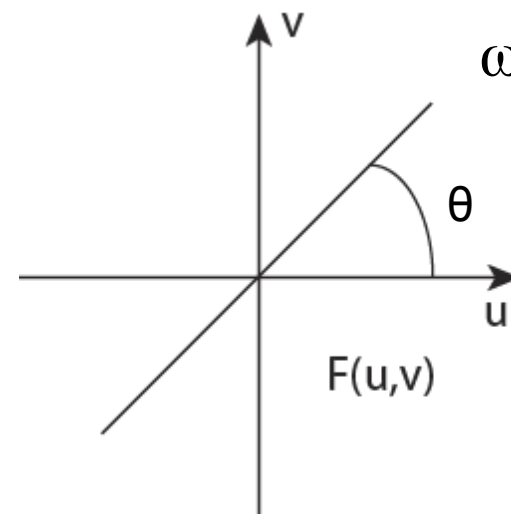
$$p_{\theta}(t) = \sin \theta \times \Lambda(t)$$

Therefore, the function in Fourier domain at **angle  $\theta = 45^0$**  is:

$$\begin{aligned} F(u, v) \big|_{\theta=45^0} &= FT_{1D}[p_{\theta=45^0}(t)] = FT_{1D}[\sin 45^0 \times \Lambda(t)] \\ &= \frac{\sqrt{2}}{2} \times \text{sinc}^2(\pi\omega) = \frac{\sqrt{2}}{2} \times \text{sinc}^2(\pi\sqrt{u^2 + v^2}) \end{aligned}$$

where  $\omega$ , in this equation, is a one-dimensional variable along the  $\theta$  direction.

$$\omega = \sqrt{u^2 + v^2}; \quad \sin 45^0 = \sqrt{2} / 2$$



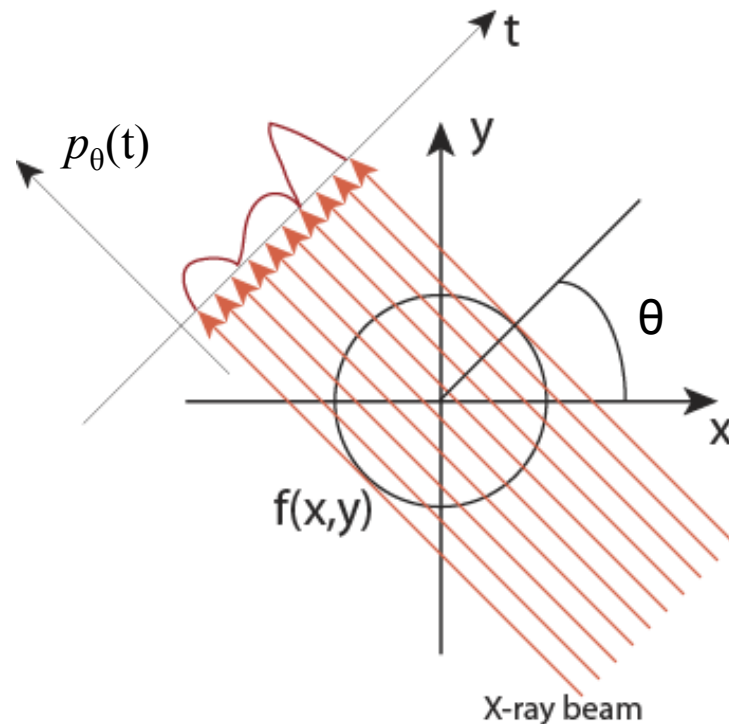
### Exercise-3:

#### CT reconstruction with Fourier transform approach

This problem is related to the CT reconstruction technique (Fourier transform approach). Suppose we have an object that has the same projection at all angles, meaning that the sinogram for all angles is the same, and can be expressed as:

$$p_{\theta}(t) = 2 \times \text{sinc}(2t)$$

Please determine the object function  $f(x, y)$  based on the Fourier slice theorem.





## Solution:

At every angle  $\theta$ , the sonogram can be expressed as:

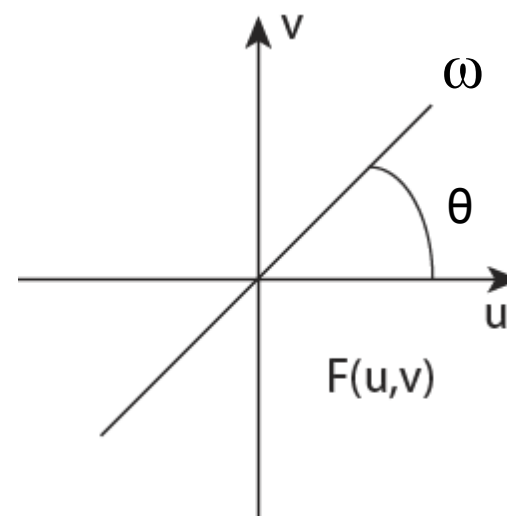
$$p_{\theta}(t) = 2 \times \text{sinc}(2t)$$

Therefore, its' 1-D Fourier transform at **every angle  $\theta$**  is:

$$P_{1D}(\omega) = FT_{1D}[p_{\theta}(t)] = \int_{-\infty}^{\infty} 2\text{sinc}(2t)e^{-i2\pi\omega t} dt = \text{rect}(\omega/2)$$

where  $\omega$ , in this equation, is a one-dimensional variable along the  $\theta$  direction.

$$\begin{aligned} \text{and } u &= \omega \cos \theta \\ v &= \omega \sin \theta \end{aligned}$$



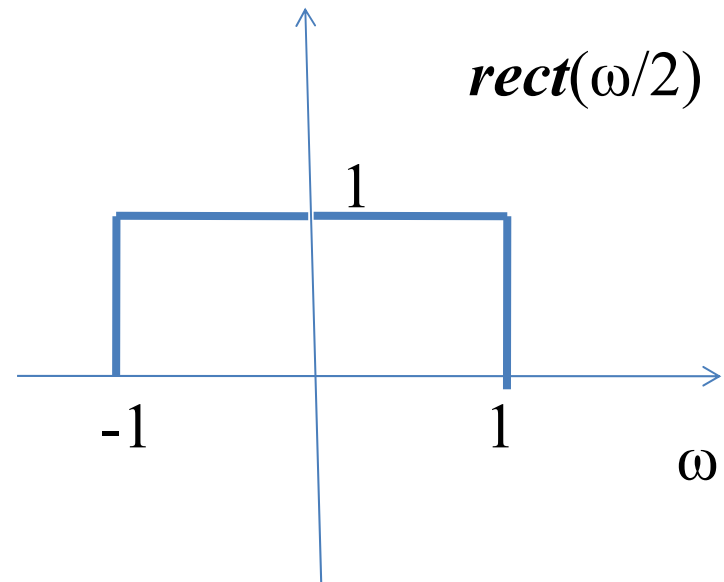
Recall Handout #02, additional notes—a brief review of *Fourier transform*:

The *1-D rect(x)* function can be expressed as:

$$\text{rect}(x) = \begin{cases} 1 & |x| \leq \frac{1}{2} \\ 0 & \text{otherwise} \end{cases}$$

Therefore, we can get *1-D rect( $\omega/2$ )*:

$$\text{rect}(\omega / 2) = \begin{cases} 1 & |\omega| \leq 1 \\ 0 & \text{otherwise} \end{cases}$$

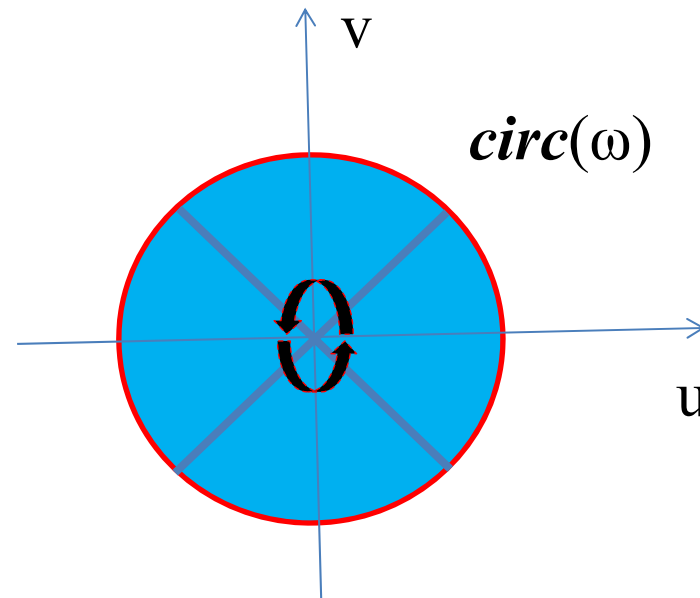


Adding up the contributions at all angles is equivalent to rotating the 1-D *rect* function over the entire range from  $\theta=0^0$  to  $\theta=180^0$ , to provide a symmetric two-dimensional frequency function (in 2-D Fourier domain)

$$F_{2D}(u, v) = \textit{circ}(\omega)$$

The *circ* function is a “pillbox” with unity radius and unity height (2-D).

$$\textit{circ}(\omega) = \begin{cases} 1 & |\omega| \leq 1 \\ 0 & \textit{otherwise} \end{cases}$$



Apply inverse Fourier transform, the 2-D object function is given by:

$$f(x, y) = FT^{-1} \{ F_{2D}(u, v) \} = \int_0^{\infty} circ(\omega) \exp^{i2\pi r \omega} 2\pi \omega d\omega$$

$$= \frac{J_1(2\pi r)}{r} = \frac{J_1(2\pi \sqrt{x^2 + y^2})}{\sqrt{x^2 + y^2}}$$

where  $r^2 = x^2 + y^2$

$J_1(2\pi r)$  is Bessel function, and  $J_1(2\pi r)/r$  is “**jinc**” function.

\* Refer to Albert Macovski, *Medical Imaging Systems*, Prentice Hall, New Jersey, 1983, p.17-18, 122

## 6.2 Hardware of CT Systems

### (1) Gantry and patient table

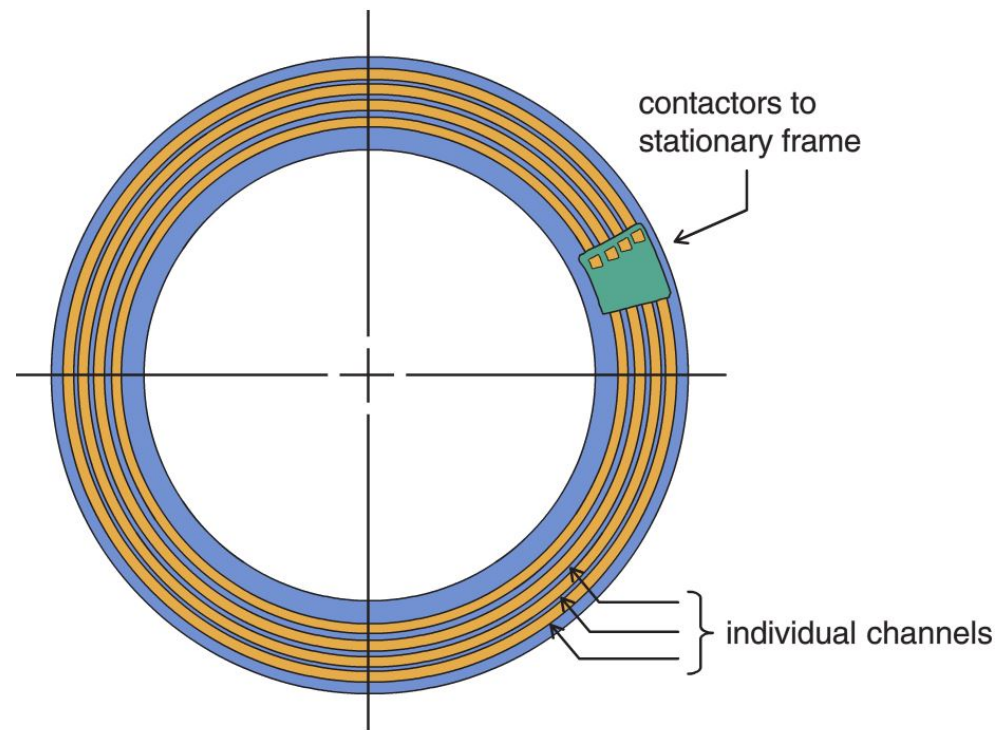
#### (a) Gantry

- ❖ The gantry provides support for the x-ray tube, detector array, and other components.
- ❖ The gantry is the moving component of the CT scanner.
- ❖ For most CT scans, a full 360-degree rotation of the CT gantry is used to collect data.



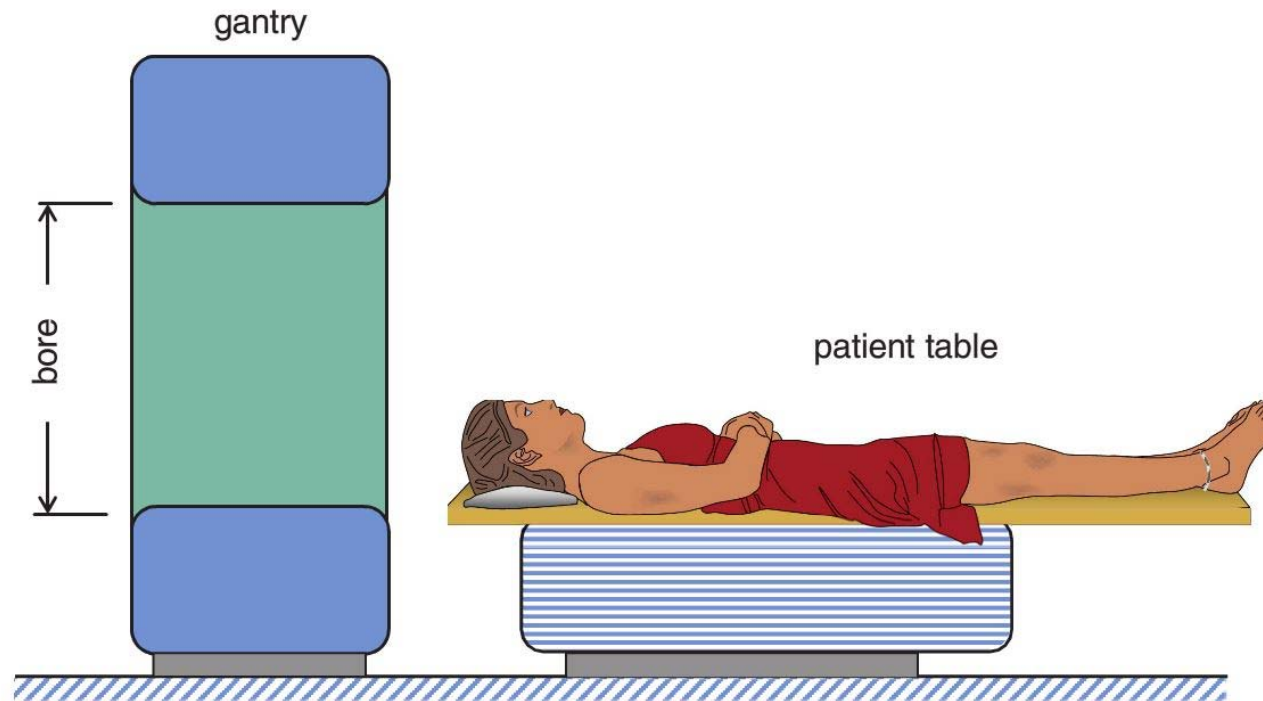
## (b) The slip ring

- ❖ Modern CT scanners use a slip ring, **electrical connection** between the stationary and the rotating frames, allowing the gantry to rotate freely, untethered to the stationary frame.

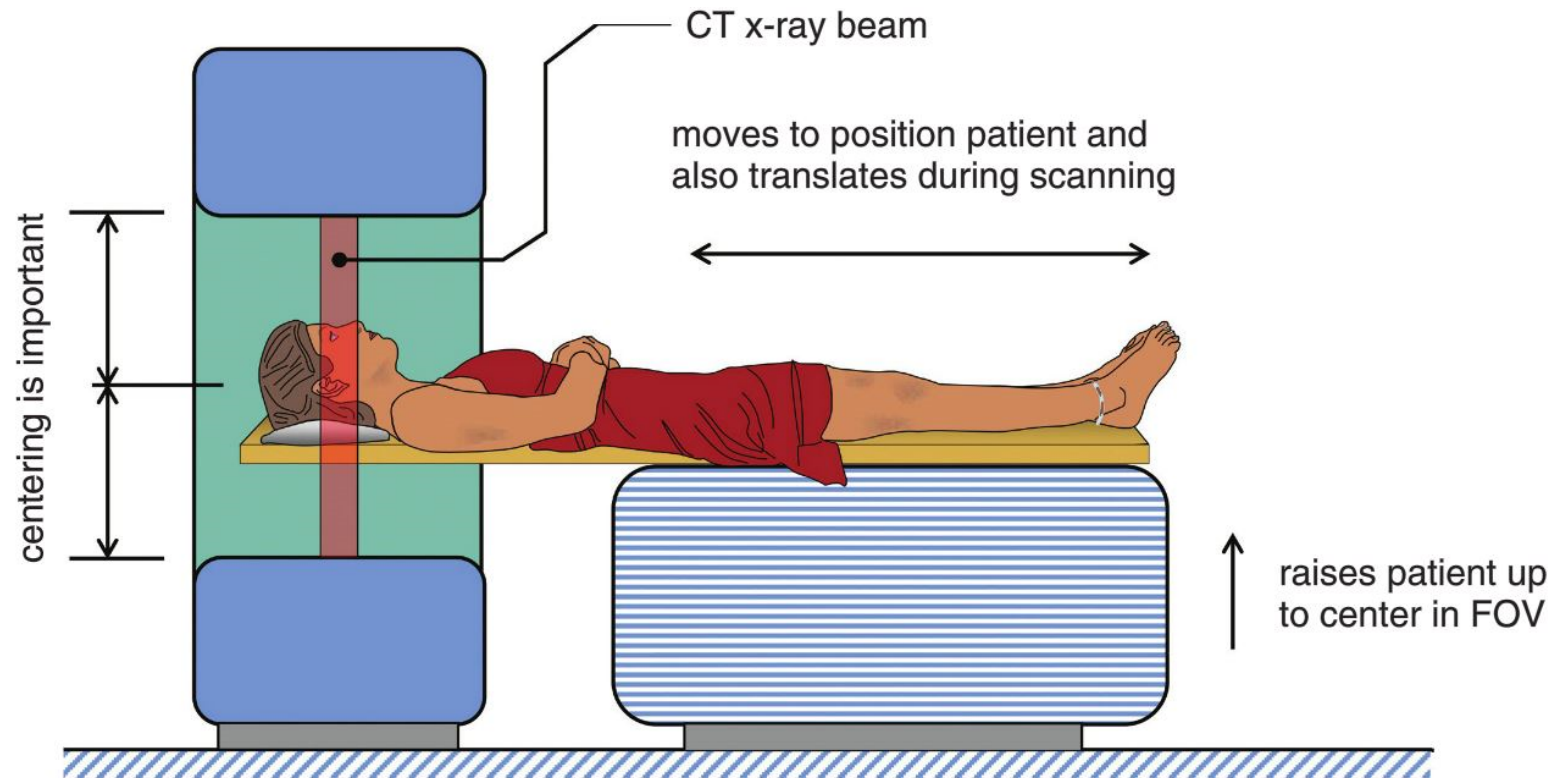


### (c) The patient table control

- ❖ The patient table is an intrinsic component of the CT scanner as well.
- ❖ The CT computer controls table motion using precision motors with telemetry feedback, for patient positioning and CT scanning.



- ❖ Under the technologist's control, the system moves the table upward and inserts the table with the patient into the bore of the scanner.



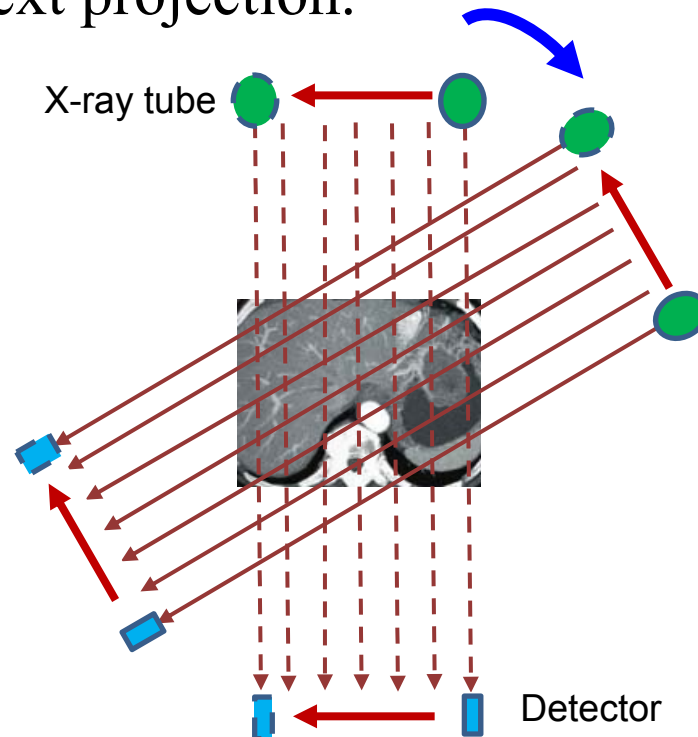
The patient table is raised and translated, allowing the patient to be inserted into the bore of the scanner. Laser lights are used for patient positioning, in all three orthogonal planes. During the actual scan, the CT imaging hardware rotates inside the gantry cover, and the table and patient translate through the bore of the gantry.



## (2) CT acquisition geometries

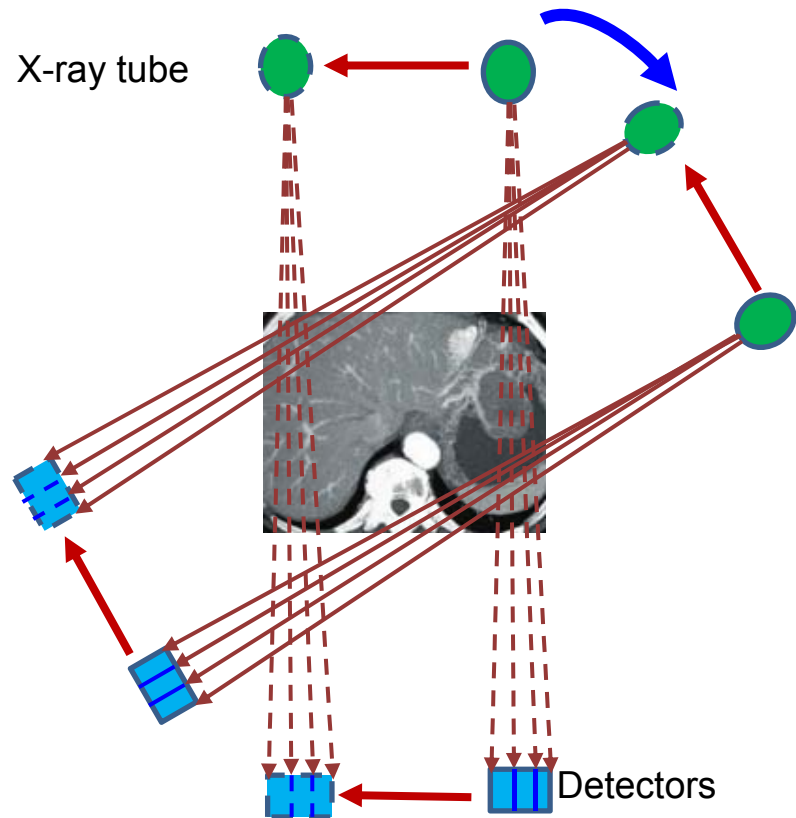
### (a) First generation—parallel beam projection

- ❖ In the first years of CT, the x-ray tube and detectors used a linear scanning trajectory.
- ❖ The source–detector combination measured parallel projections, one sample at a time, by **stepping linearly across object**.
- ❖ After each projection, the gantry rotated to a new position for the next projection.



- One detector
- Translation-rotation
- Parallel beam

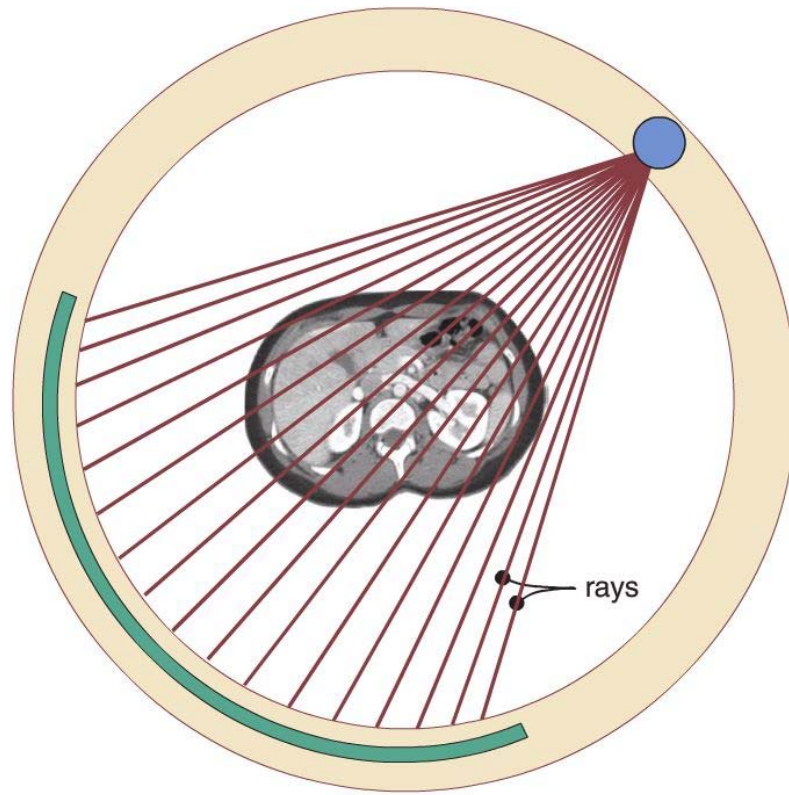
## (b) Second generation—small fan beam



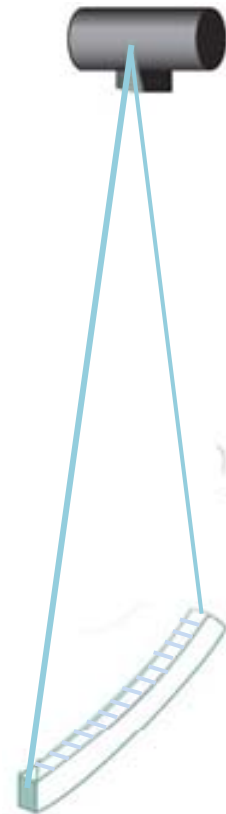
- Multiple detectors
- Translation-rotation
- Small fan beam angle

### (c) Third generation—large fan beam

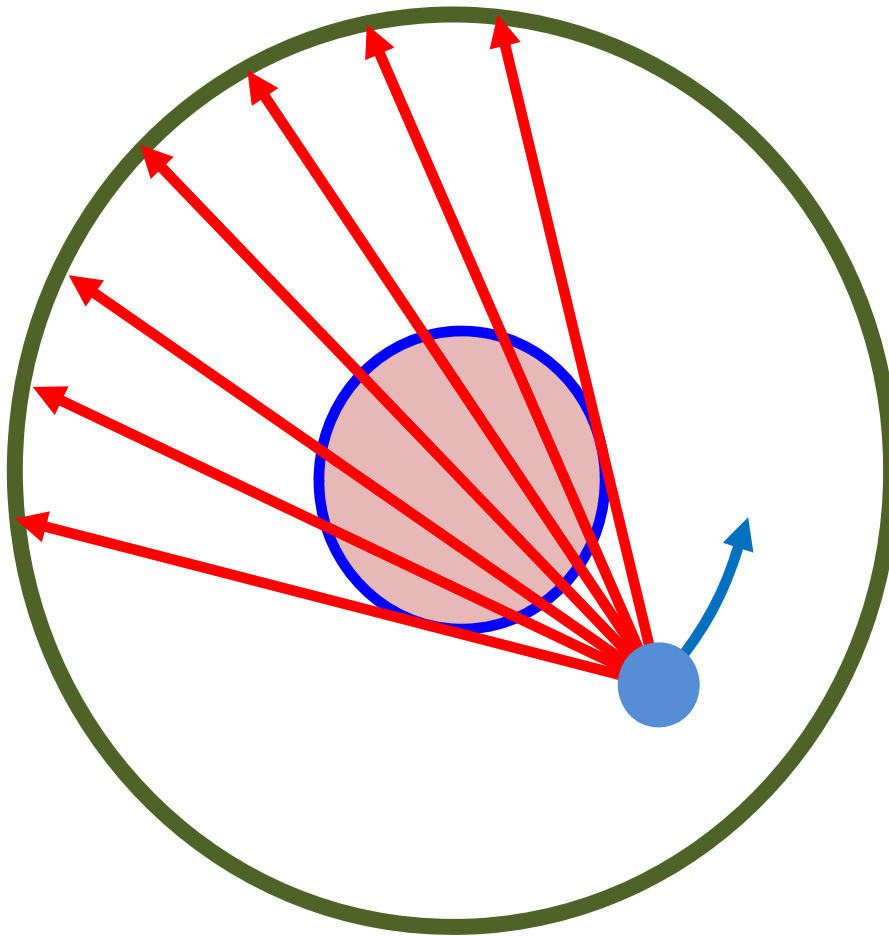
- ❖ The newer CT uses large fan beam projection, wide enough to encompass the entire region of interest.
- ❖ The x-ray tube and a single row (**single-slice**) of multiple detectors rotate together about the patient.



fan beam projection



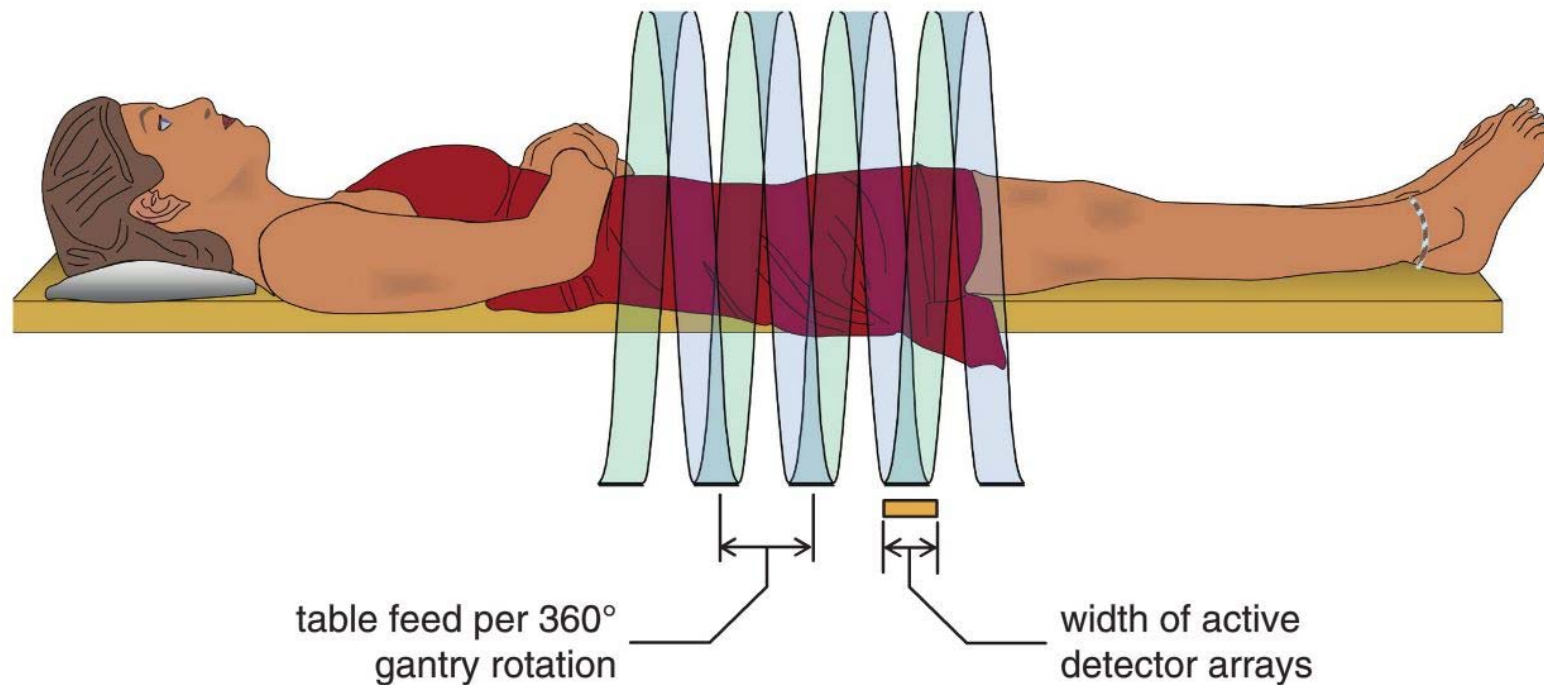
**(d) Fourth generation—large fan beam**



- Detector ring
- Source-rotation
- Large fan beam angle

### (e) Modern CT system—helical /spiral CT

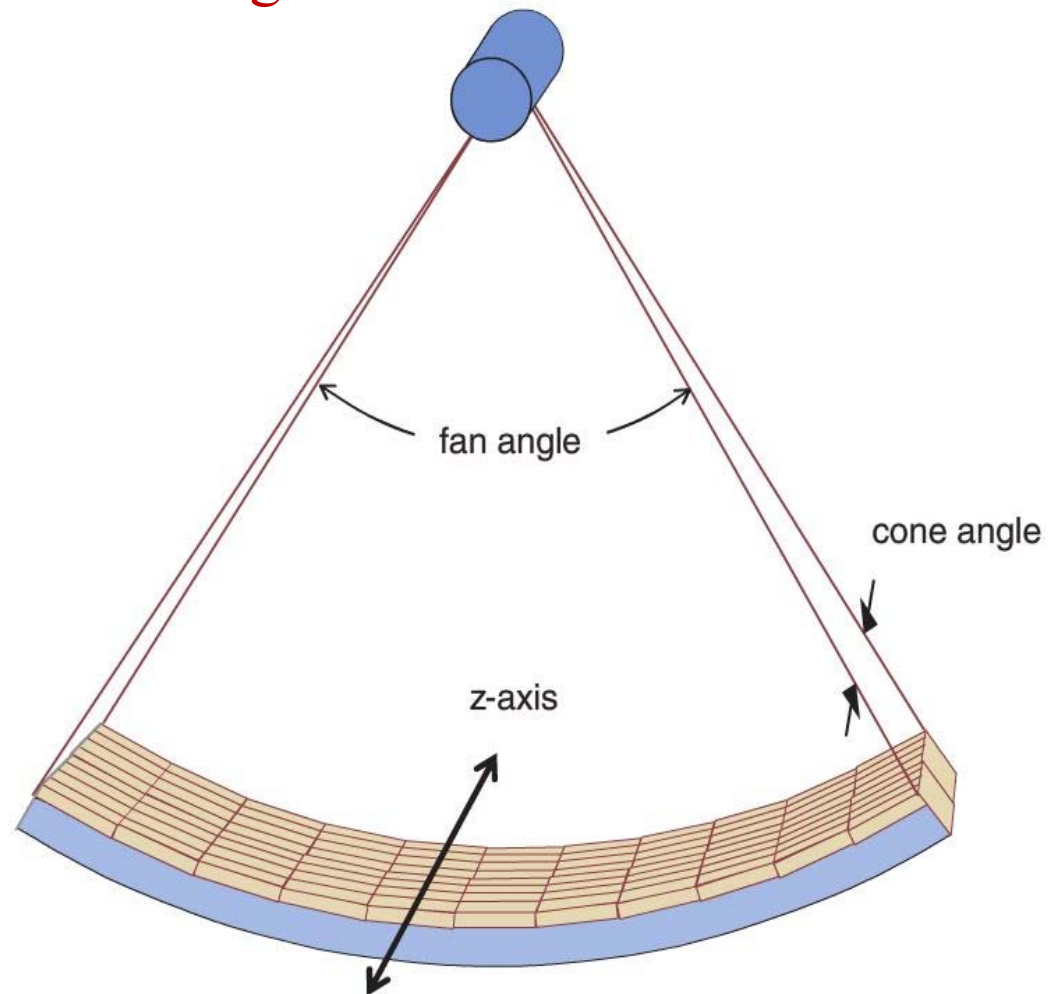
- ❖ With helical (also called spiral) scanning, the table moves at a constant speed while the gantry rotates around the patient.
- ❖ With helical CT scanning, the x-ray tube has a helical trajectory around the patients.



The helical (or spiral) CT scanning.

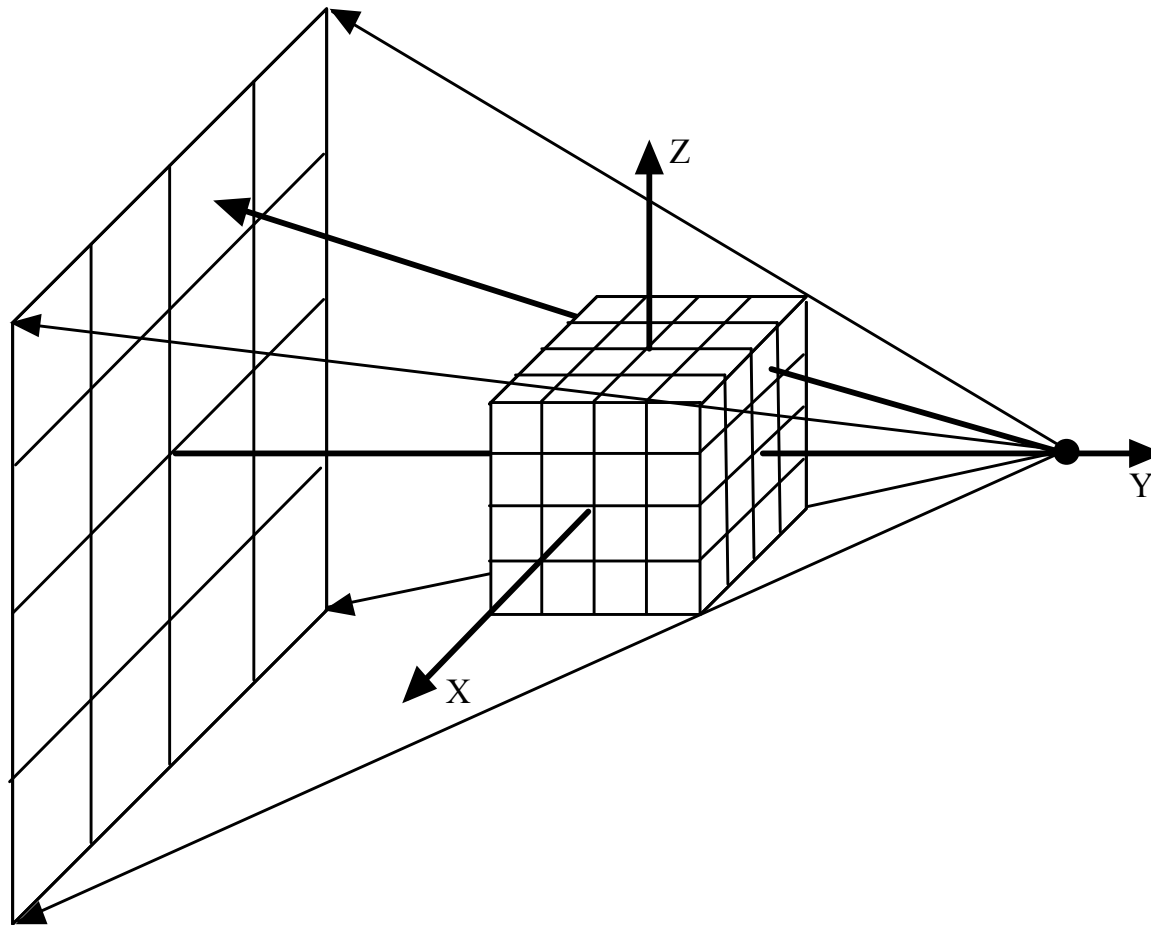
## (f) Modern CT system—multi-slices CT

- ❖ Uses multiple row of detectors (multi-slices CT)
- ❖ With a **cone beam angle**.

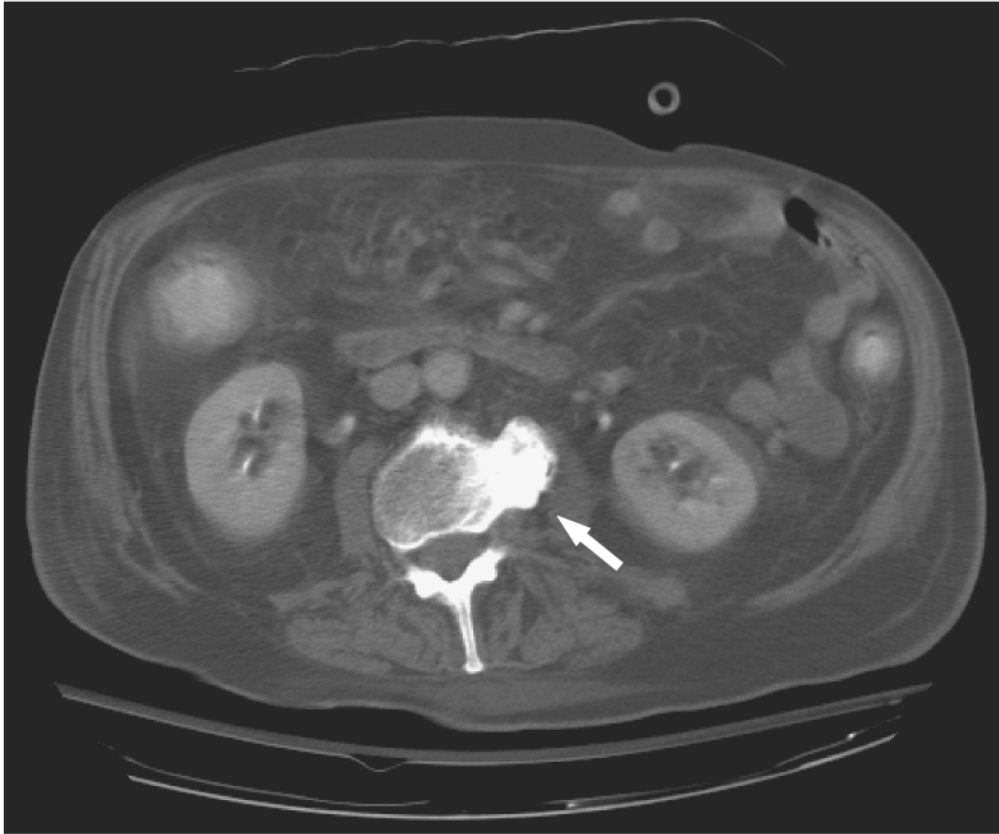


### (g) Large cone beam geometry

- ❖ The cone angle and the detector array is large enough for acquiring the entire data set without table translation
- ❖ For some applications



## Computed tomography



J.T. Bushberg, J.A. Seibert, E.M. Leidholdt, Jr., J.M. Boone, *The Essential Physics of Medical Imaging*, 2002

- ❖ A computed tomography, (CT) image of the abdomen reveals a ruptured disc (arrow) manifested as the bright area of the image adjacent to the vertebral column. Anatomic structures such as the kidneys, arteries, and intestines are clearly represented in the image.
- ❖ CT provides high-contrast sensitivity for soft tissue, bone, and air interfaces without superimposition of anatomy.



## 6.3. Image Quality

**(1) Resolution:** depends on: detector aperture size, spatial sampling rate, x-ray tube focal spot size, and reconstruction algorithm.

Consider: (a) resolution within each transverse plane; and (b) resolution in the direction perpendicular to those planes (slice thickness).

**(2) Noise:** depends on x-ray quantum noise, electronic noise should be considered too.

**(3) Radiation dose** considerations

## Summary:

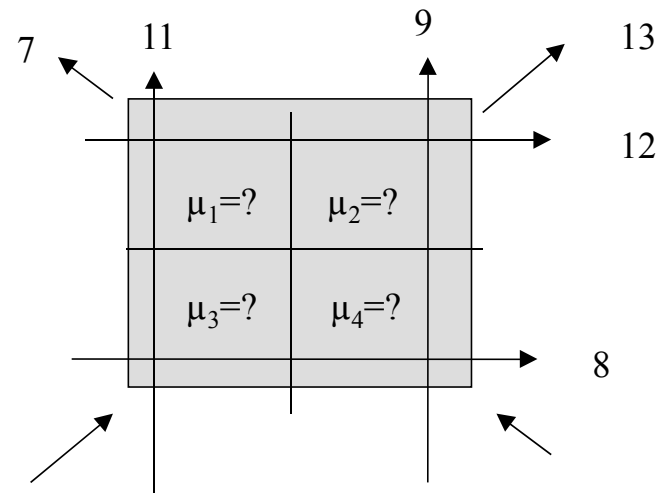
1. Computed tomography maps the linear attenuation coefficients throughout a transverse slice of tissue (or an object).
  - ❖ The principles of CT are conceptually simple.
  - ❖ Physically, x-rays can traverse a cross-section of an object along straight lines, be attenuated by the object, and detected outside it.
  - ❖ During CT scanning, the cross-section is probed with x-rays from various directions, attenuated signals are recorded and converted to projections of the linear attenuation coefficient distribution of the cross-section.
  - ❖ These x-ray shadows are directly related to the Fourier transform of the cross-section, and can be processed to reconstruct the cross-section.
2. Concepts of Voxel, CT number
3. Reconstruction techniques – filtered back projection

## References:

- ❑ J. Hsieh, <<Computed Tomography: Principles, Design, Artifacts, and recent Advances>>, SPIE Press, 2002.
- ❑ Liang Li, Zhiqiang Chen, and Ge Wang, “Reconstruction Algorithms”, Chapter 03, <<Cone Beam Computed Tomography>>, Edited by Chris C. Shaw, CRC Press, 2014
- ❑ Robert Cierniak, <<X-Ray Computed Tomography in Biomedical Engineering>>, Springer, 2011

## Homework # 5

1. If the linear attenuation coefficient of air under a specific x-ray technique (KVp) is zero, ( $\mu_{\text{air}} = 0 \text{ cm}^{-1}$ ), What is the CT number of air?
2. Assume a mono-energetic x-ray source for which  $\mu_{\text{water}} = 0.2 \text{ cm}^{-1}$ . If a lesion has a linear attenuation coefficient 10% higher than that of water, then what will be the lesion's CT number?
3. Suppose we are imaging a body slice that consists of four voxels of unit dimension ( $\Delta x=1$ ). The ray sums were measured and are given by the following diagram. Try to determine linear attenuation coefficient of each voxel with algebraic reconstruction technique (ART). Please show each step of iterations.



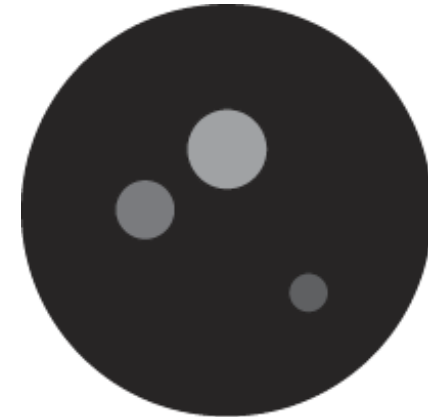
4. This problem is related to the CT reconstruction technique (Fourier Transform approach). Assuming that a series of projections from  $0^\circ$  to  $180^\circ$  at  $1^\circ$  increments; resulted a Sinogram that can be expressed as:

$$P_\theta(t) = 4 \times \sin \theta \times \text{rect}(3t)$$

Based on Fourier slice theorem, please determine the mathematical expression of the function in Fourier domain at  $\theta=60^\circ$ .

### 5. An exercise in CT projection and reconstruction with

**Matlab:** The cross-section of an object with three holes of different sizes and materials (different attenuation under x-ray) is shown by the figure. The numerical value of each of the 256 by 256 voxels is given in an attached file named "cross-section.dat". The numerical values are related to the linear attenuation coefficients of the object under a specific x-ray for the purpose of this exercise.



The cross-section of the target object with three holes

- (a) Using Matlab function “radon”, determine and print the sinograms resulted from the following sets of projection angles:
  - (0, 1, 2, 3, ..., 179, with 1 degree increment
  - (0, 5, 10, 15, ..., 175; with 5 degree increment
  - (0, 30, 60, ..., 150; with 30 degree increment
- (b) Using Matlab function “iradon”, reconstruct and print the CT slices from the sinograms obtained in (a), respectively.

Note: The following flow chart may be helpful. You can also refer to Matlab Help about “radon” and “iradon” for their respective usage.

## Flowchart for CT projection and reconstruction exercise with Matlab

